



# Behavior of halogens during the degassing of felsic magmas

Hélène Balcone-Boissard, Benoît Villemant, Georges Boudon

## ► To cite this version:

Hélène Balcone-Boissard, Benoît Villemant, Georges Boudon. Behavior of halogens during the degassing of felsic magmas. *Geochemistry, Geophysics, Geosystems*, 2010, 11, pp.Q09005. 10.1029/2010GC003028 . hal-00536620

**HAL Id: hal-00536620**

**<https://hal.science/hal-00536620>**

Submitted on 9 Jun 2017

**HAL** is a multi-disciplinary open access archive for the deposit and dissemination of scientific research documents, whether they are published or not. The documents may come from teaching and research institutions in France or abroad, or from public or private research centers.

L'archive ouverte pluridisciplinaire **HAL**, est destinée au dépôt et à la diffusion de documents scientifiques de niveau recherche, publiés ou non, émanant des établissements d'enseignement et de recherche français ou étrangers, des laboratoires publics ou privés.



## Behavior of halogens during the degassing of felsic magmas

**H. Balcone-Boissard**

*ISTeP, CNRS UMR 7193, UPMC Université Paris 6, Case courrier 129, 4 place Jussieu, F-75252 Paris, France (helene.balcone-boissard@upmc.fr)*

**B. Villemant**

*ISTeP, CNRS UMR 7193, UPMC Université Paris 6, Case courrier 129, 4 place Jussieu, F-75252 Paris, France*

*Institut de Physique du Globe de Paris et Université Paris Diderot (Sorbonne Paris-Cité), CNRS UMR 7154, 1, rue Jussieu, F-75238 Paris CEDEX 05, France*

**G. Boudon**

*Institut de Physique du Globe de Paris et Université Paris Diderot (Sorbonne Paris-Cité), CNRS UMR 7154, 1, rue Jussieu, F-75238 Paris CEDEX 05, France*

[1] Residual concentrations of halogens (F, Cl, Br, I) and H<sub>2</sub>O in glass (matrix glass and melt inclusions) have been determined in a series of volcanic clasts (pumice and lava-dome fragments) of plinian, vulcanian and lava dome-forming eruptions. Felsic magmas from calc-alkaline, trachytic and phonolitic systems have been investigated: Montagne Pelée and Soufrière Hills of Montserrat (Lesser Antilles), Santa Maria-Santiaguito (Guatemala), Fogo (Azores) and Vesuvius (Italy). The behavior of halogens during shallow H<sub>2</sub>O degassing primarily depends on their incompatible character and their partitioning between melt and exsolved H<sub>2</sub>O vapor. However, variations in pre-eruptive conditions, degassing kinetics, and syn-eruptive melt crystallization induce large variations in the efficiency of halogen extraction. In all systems studied, Cl, Br and I are not fractionated from each other by differentiation or by degassing processes. Cl/Br/I ratios in melt remain almost constant from the magma reservoir to the surface. The ratios measured in erupted clasts are thus characteristic of pre-eruptive magma compositions and may be used to trace deep magmatic processes. F behaves as an incompatible element and, unlike the other halogens, is never significantly extracted by degassing. Cl, Br and I are efficiently extracted from melts at high pressure by H<sub>2</sub>O-rich fluids exsolved from magmas or during slow effusive magma degassing, but not during rapid explosive degassing. Because H<sub>2</sub>O and halogen mobility depends on their speciation, which strongly varies with pressure in both silicate melts and exsolved fluids, we suggest that the rapid pressure decrease during highly explosive eruptions prevents complete equilibrium between the diverse species of the volatiles and consequently limits their degassing. Conversely, degassing in effusive eruptions is an equilibrium process and leads to significant halogen output in volcanic plumes.

**Components:** 13,500 words, 5 figures, 4 tables.

**Keywords:** halogens; felsic melts; eruptive style; speciation.

**Index Terms:** 1065 Geochemistry: Major and trace element geochemistry; 8499 Volcanology: General or miscellaneous.

**Received** 4 January 2010; **Revised** 28 May 2010; **Accepted** 9 June 2010; **Published** 9 September 2010.

Balcone-Boissard, H., B. Villemant, and G. Boudon (2010), Behavior of halogens during the degassing of felsic magmas, *Geochem. Geophys. Geosyst.*, 11, Q09005, doi:10.1029/2010GC003028.

## 1. Introduction

[2] The halogens F, Cl, Br, and I behave simply during magmatic differentiation and degassing because they generally have low mineral/melt partition coefficients and high H<sub>2</sub>O vapor-melt partition coefficients. Pre-eruptive, highly differentiated magmas (rhyolitic, trachytic, or phonolitic melts) generally have high H<sub>2</sub>O concentrations but low CO<sub>2</sub> or SO<sub>2</sub> concentrations because of the much lower solubility of these volatile components compared to H<sub>2</sub>O [Morizet *et al.*, 2002]. Experimental data show that in such highly differentiated melts halogens are highly soluble and that their volatile behavior is mainly controlled by H<sub>2</sub>O degassing [Métrich and Rutherford, 1992; Webster, 1997; Webster *et al.*, 1999; Bureau *et al.*, 2000; Bureau and Métrich, 2003; Moretti *et al.*, 2003; Carroll, 2005; Gardner *et al.*, 2006; Chevychev *et al.*, 2008]. Reconstruction of the melt degassing history may be carried out by relating the halogen concentration in glass with the corresponding vesicularity and crystallinity of magma fragments quenched at different degassing steps. As accurate measurements of H<sub>2</sub>O concentrations in glass of erupted material (melt inclusions, matrix glass) are often difficult, halogens may represent a good alternative to identify and trace degassing processes.

[3] In this paper, we compare halogen concentrations in eruptive products from a set of plinian and lava dome-forming eruptions involving various types of felsic melts. This assessment allows us to establish general rules for halogen behavior during magma degassing as a function of melt composition, pre-eruptive conditions and eruptive style.

[4] The investigated eruptions are the Fogo A eruption of Fogo volcano (~4700 a BP, São Miguel, Azores), the P1 eruption at Montagne Pelée (650 a BP, Martinique), the 1902, 1929 and present-day eruptions at Santa Maria-Santiago (Guatemala), the 1995-present-day eruption at Soufrière Hills (Montserrat) and the 79 AD Vesuvius eruption (Italy). These examples cover a large range of felsic melt compositions, from rhyolitic (Montagne Pelée, Soufrière Hills, Santa Maria-Santiago), to trachytic (Fogo) and phonolitic (Vesuvius) and a large variety of eruptive styles, including plinian eruptions (Fogo, Santa Maria, Montagne Pelée, Vesuvius), lava dome-forming eruptions (Santiago, Montagne Pelée, Soufrière Hills) and vulcanian explosions (Soufrière Hills).

[5] New halogen (F, Cl, Br, I) and H<sub>2</sub>O concentrations in volcanic clasts are reported for Fogo, Montagne Pelée and Santa Maria-Santiago volcanoes. They are compared with previously published data on Vesuvius [Balcone-Boissard *et al.*, 2008], Soufrière Hills (the ongoing eruption since 1995 [Villemant *et al.*, 2008]), Montagne Pelée, and Santa Maria-Santiago [Villemant and Boudon, 1998, 1999; Villemant *et al.*, 2003].

## 2. Materials and Analytical Methods

[6] The detailed reconstruction of the degassing processes for each eruptive unit is based on a systematic collection of volcanic clasts and, for each individual clast, on analyses of textural characteristics (vesicularity, microcrystallinity) and volatile concentrations in the matrix glass and glassy melt inclusions, which represent the pre-eruptive melt in the magmatic system. This method combined with modeling has been successfully applied to interpret other eruptions [Villemant and Boudon, 1998, 1999; Villemant *et al.*, 1996, 2003, 2008; Balcone-Boissard *et al.*, 2008].

### 2.1. Volcanic Eruptions

[7] The products of six characteristic eruptions from five volcanoes in different geodynamic settings were studied. Three eruptions are from calc-alkaline volcanoes from subduction zones. Montagne Pelée (Martinique) and Soufrière Hills Volcano (Montserrat) in the Lesser Antilles arc result from the subduction of the Atlantic oceanic crust of the North American plate under the Caribbean plate whereas Santa Maria-Santiago (Guatemala) is associated with the subduction of the Cocos plate beneath the Caribbean plate. Vesuvius (Italy) is located in a complex geodynamic system and erupted magmas are silica-undersaturated and highly potassic (tephri-phonolitic to phonolitic). Fogo (São Miguel, Azores (37°–40° N)), is located in the Atlantic Ocean on the triple junction where the Eurasian, African and American plates converge; erupted magmas are trachytic in composition.

[8] Montagne Pelée is one of the most active volcanoes of the Lesser Antilles arc. The last plinian eruption (P1, 650 y BP old), hereafter referred as Montagne Pelée, was studied. It is a complex eruption that began with effusion of a lava-dome that was later destroyed by two directed lateral explosions that generated two dilute pyroclastic

density currents on the western flank of the volcano. It was immediately followed by a plinian eruption characterized by a succession of sustained plinian activity and plinian column collapse phases [Villemant and Boudon, 1998]. Dense clasts from the lava-dome, clasts from the pyroclastic density current deposits and clasts in the pumice fallout deposits were studied [Villemant and Boudon, 1999].

[9] Soufrière Hills volcano on the island of Montserrat, in the northern part of the Lesser Antilles arc, has been active since 1995. This eruption (hereafter referred to as Montserrat) is one of the most complex eruptions observed in recent decades, consisting of a succession of lava domes, vulcanian explosions, flank-collapse and dome-collapse events [Sparks et al., 1998; Voight et al., 1999; Robertson et al., 1998, 2000]. Dense clasts from the first phase of lava dome growth and pumice clasts from the 1997 vulcanian explosions were studied [Villemant et al., 2008].

[10] The October 1902 plinian eruption of Santa Maria volcano (Guatemala) was one of the largest eruptions of the last century [Williams and Self, 1983; Rose, 1972a]. This eruption, hereafter referred to as Santa Maria, generated a thick pumice fallout deposit followed by caldera collapse in which, 20 years later, Santiaguito volcano was emplaced and continues to be permanently active [Rose, 1972b]. This activity, hereafter referred to as Santiaguito, consists in a series of lava domes, which underwent numerous explosion and collapse events [Rose, 1972b; Harris et al., 2003]. Pumice clasts from the plinian phase of the Santa Maria volcano and clasts from different lava domes of Santiaguito were studied (samples covering the period 1947–1989) (Santa Maria-Santiaguito samples [Villemant et al., 2003]).

[11] The 79 AD eruption of Vesuvius, also known as the “Pompeii eruption” and hereafter referred to as Vesuvius, is commonly divided into three phases [Sigurdsson et al., 1990; Cioni et al., 1995]: an initial phreatomagmatic phase followed by a plinian event that produced a thick pumice fallout deposit and a final phase dominated by numerous column collapse events. The magma erupted during the plinian phase varies in composition from phonolite to less differentiated phonolite. This change in composition corresponds to a sharp transition in the tephra fallout deposit from the “white pumice” to the “grey pumice.” Studies dedicated to this eruption include determination of pre-eruptive conditions and magma degassing [Cioni, 2000;

Signorelli and Capaccioni, 1999] and textures and vesicularity [Gurioli et al., 2005]. The behavior of halogens during the evolution of this eruption was studied in detail by Balcone-Boissard et al. [2008]. Here we focus only on white pumice units, although we briefly consider the distinction between three eruptive units.

[12] Fogo volcano is one of the three active stratovolcanoes of São Miguel island, in the Azores archipelago [Moore, 1990; Booth et al., 1978]. The last eruption of Fogo occurred in 1563 AD, but the most important plinian eruption, the Fogo A eruption, is dated at ~4700 y BP [Snyder et al., 2007]. It is hereafter referred to as the Fogo A eruption. The magma erupted is trachytic in composition. The main plinian phase produced a pumice fallout layer in which several ash-and-pumice flow and surge deposits intercalate, attesting to several collapses of the eruptive column during the eruption [Walker and Croasdale, 1971]. Snyder et al. [2004] and Widom et al. [1992] provide petrogenetic models of the Fogo A magmatic evolution, based on chemical, textural and isotopic data, and the deposits represent the upper part of a chemically zoned magma reservoir [Watanabe et al., 2005; Snyder et al., 2007]. Cruz et al. [2004] performed a detailed study of the vesicularity and volatile concentration (H<sub>2</sub>O, F, Cl) of the eruption products. The pre-eruptive water concentration was estimated by Wolff and Storey [1983]. Here we focus on the main plinian phase. When necessary, the distinction between three eruptive unit included in the main plinian fallout is considered.

## 2.2. Major Element Composition of Glass

[13] Whole-rock, major-element compositions were measured by ICP-AES (SARM, CRPG Nancy, France). Matrix glass compositions (major and volatile concentrations) were measured by electron probe micro-analysis (EPMA, Cameca SX 100, Camparis, Université Paris VI). The thorium concentrations in samples from the Fogo A eruption was measured by ICP-MS (Thermo-Optek ICP-MS at Université de Paris VI).

[14] All studied magmas are silica-rich (SiO<sub>2</sub> > 55 wt%) and correspond to low temperature (800–900°C) differentiated melts. In the alkaline systems investigated, whole rock and matrix glass compositions are very similar due to the low phenocryst content, whereas the calc-alkaline magmas consist of rhyolitic melts with large amounts of phenocrysts. For each studied calc-alkaline eruption, the melt composition remains homogeneous through-

**Table 1.** Whole Rock and Matrix Glass Compositions (Anhydrous Basis) of the Studied Eruptions<sup>a</sup>

Vesuvius						
	Whole Rock-Plinian Clasts (WP, 6 Analyses)			Matrix Glass (43 Analyses)		
	Composition	sabs		Composition	sabs	
SiO <sub>2</sub>	55.66	0.7		55.88	0.8	
TiO <sub>2</sub>	0.23	0.1		0.22	14.5	
Al <sub>2</sub> O <sub>3</sub>	22.15	0.3		23.06	0.9	
Fe <sub>2</sub> O <sub>3</sub>	2.55	0.1		2.45	3.1	
MnO	0.13	0.3		0.16	0.0	
MgO	0.30	0.1		0.10	10.5	
CaO	3.32	0.3		3.04	5.7	
Na <sub>2</sub> O	5.78	0.2		7.18	1.8	
K <sub>2</sub> O	9.83	0.2		7.81	0.9	
P <sub>2</sub> O <sub>5</sub>	0.05	0.1		0.09	0.1	
Total	100.0			100.0		
Fogo A						
	Whole Rock-Plinian Clasts (Main, 4 Analyses)			Matrix Glass (16 Analyses)		
	Composition	sabs		Composition	sabs	
SiO <sub>2</sub>	65.50	0.8		64.56	0.7	
TiO <sub>2</sub>	0.44	0.1		0.49	13.0	
Al <sub>2</sub> O <sub>3</sub>	16.80	0.3		16.98	1.5	
Fe <sub>2</sub> O <sub>3</sub>	3.57	0.1		3.54	6.4	
MnO	0.22	0.3		0.21	11.9	
MgO	0.23	0.1		0.32	41.2	
CaO	0.76	0.1		0.90	28.2	
Na <sub>2</sub> O	6.72	0.2		7.20	2.9	
K <sub>2</sub> O	5.69	0.2		5.80	2.1	
P <sub>2</sub> O <sub>5</sub>	0.07	0.1		n.a.	n.a.	
Total	100.0			100.0		
Montagne Pelée						
	Whole Rock-Plinian Clasts (11 Analyses)		Whole Rock-Lava-Dome Fragments (5 Analyses)		Matrix Glass (10 Analyses)	
	Composition	sabs	Composition	sabs	Composition	sabs
SiO <sub>2</sub>	61.5	1.0	60.4	1.0	75.31	0.6
TiO <sub>2</sub>	0.5	3.7	0.5	5.9	0.22	8.9
Al <sub>2</sub> O <sub>3</sub>	17.6	1.4	17.8	1.1	13.31	1.1
Fe <sub>2</sub> O <sub>3</sub>	7.1	3.1	7.3	3.0	2.71	2.9
MnO	0.2	6.1	0.2	6.2	0.00	0.0
MgO	2.3	3.7	2.4	5.6	0.32	9.8
CaO	6.5	3.3	6.8	4.5	2.51	5.5
Na <sub>2</sub> O	3.3	3.9	3.4	1.1	3.25	8.4
K <sub>2</sub> O	1.0	3.8	0.9	3.3	2.17	3.4
P <sub>2</sub> O <sub>5</sub>	0.2	5.4	0.2	5.3	0.2	5.1
Total	100.0	0.2	100.0	0.5	100.0	



**Table 1.** (continued)

Santa Maria-Santiaguito						
Whole Rock-Plinian Clasts (9 Analyses)			Whole Rock-Lava-Dome Fragments (11 Analyses)		Matrix Glass (13 Analyses)	
Composition		sabs	Composition		Composition	sabs
SiO <sub>2</sub>	66.9	1.8	64.7	2.2	73.52	0.8
TiO <sub>2</sub>	0.3	13.7	0.4	19.4	0.16	14.1
Al <sub>2</sub> O <sub>3</sub>	16.7	1.6	17.2	2.0	15.43	1.2
Fe <sub>2</sub> O <sub>3</sub>	3.8	13.4	4.5	12.2	1.91	14.5
MnO	0.1	4.6	0.1	3.5	0.00	0.0
MgO	1.2	23.5	1.6	17.9	0.48	12.2
CaO	4.1	11.7	4.8	10.8	2.18	10.8
Na <sub>2</sub> O	4.9	4.0	4.8	3.8	3.48	11.7
K <sub>2</sub> O	1.8	8.7	1.7	11.4	2.64	2.8
P <sub>2</sub> O <sub>5</sub>	0.2	3.5	0.2	8.6	0.2	5.3
Total	100.0		100.0		100.0	

<sup>a</sup>Whole rock compositions: ICP-AES (SARM, Nancy-France). Matrix glass compositions: EPMA (SX100, Camparis, France). sabs: standard deviation; n: number of analyses. The absolute sigma is in percentage.

out the whole eruptive sequence, irrespective of the eruptive style whereas in alkaline systems large variations in composition may be observed (Table 1).

### 2.3. Volatile Concentrations of Volcanic Clasts

[15] Representative clasts of each example were powdered in an agate mortar for bulk chemical analyses. Whole rock volatile concentrations (H<sub>2</sub>O, CO<sub>2</sub>) were measured by H<sub>2</sub> and CO<sub>2</sub> manometry after vacuum extraction under reducing conditions for H<sub>2</sub>O and using a temperature trap to separate CO<sub>2</sub>. These techniques provide good analytical precisions: <10% for H<sub>2</sub>O and CO<sub>2</sub>. In all volcanic systems, H<sub>2</sub>O represents the main volatile component; magmatic CO<sub>2</sub> is negligible and will not be considered further in this contribution. Data are reported in auxiliary material Data Sets S1 and S2.<sup>1</sup>

[16] Halogens in the groundmass were extracted from bulk powders of volcanic clasts by pyrohydrolysis and analyzed by ion chromatography for F and Cl and by ICP-MS for Br and I [Michel and Villemant, 2003; Balcone-Boissard *et al.*, 2009]. These techniques provide good analytical precision: <10% for F and Cl and ~10% for Br (both are relative %). For I, the precision is ~10–20% (relative), due to the low I abundance (~10–200 ppb) and analytical difficulties (volatility, contamination) (as detailed by Balcone-Boissard *et al.* [2009]). Residual H<sub>2</sub>O and halogens are concentrated as

dissolved species in matrix glass in all samples studied. Phenocrysts are produced by magmatic differentiation in the reservoir, at depth, and are not linked to the degassing history. Estimates of volatile concentrations in the groundmass are obtained by correcting the bulk chemical analyses by the phenocryst weight fraction and, in some cases, from the volatile concentrations of volatile-bearing phenocrysts (such as amphiboles in the case of Montserrat [Villemant *et al.*, 2008]). These compositions then represent the melt composition in magma chamber and conduit during degassing and eruption. The phenocryst weight fraction in each clast is obtained by mass balance calculations using major and trace element compositions measured by EPMA and ICP-MS in separated groundmass, phenocrysts and whole rocks [Balcone-Boissard *et al.*, 2009]. This method provides more reliable values than point counting or image analysis [Villemant *et al.*, 2003]. For low phenocryst concentrations (<10 wt% relative), this correction is within the analytical error. These corrections do not modify the relative abundances of volatiles, except in the case of large abundances of volatile-bearing phenocrysts. Thus, characteristic abundance ratios such as Cl/F, Cl/Br or Br/I in residual glasses and/or the groundmass may be calculated from bulk rock analysis without introduction of other sources of error from the correction of phenocryst concentration.

[17] In recent years, considerable effort has been spent developing analysis techniques for volatiles in volcanic glasses (matrix glass and melt inclusion). EPMA is the most widespread technique for

<sup>1</sup>Auxiliary materials are available at <ftp://ftp.agu.org/apend/gc/2010gc003028>.

F and Cl measurements. A routine dedicated to halogen measurements in volcanic glasses (melt inclusions and matrix glass) has been developed using a Cameca SX100 microprobe (Camparis, Université Paris VI) that ensures good analytical precision (10% and 5% relative for F and Cl, respectively) and low detection limits (120 ppm for F and 30 ppm for Cl). Details of the chemical analysis procedures are given by *Balcone-Boissard et al.* [2008]. Point analyses and textural investigations were performed on one part of a representative clast that was embedded in epoxy resin, ground and polished. Analyses of major elements were performed with an acceleration voltage of 15 kV and a beam current of 4 nA. The dwell time was 10s, except for Si (5s) and Na (5s). F and Cl were measured with a dwell time of 120s and 90s respectively, an acceleration voltage of 15 kV and a beam current of 100 nA. Analytical conditions (in particular dwell times) were chosen to ensure no significant Na or F diffusion during EPMA analyses, as monitored using glass standards. For intercalibration of EPMA and pyrohydrolysis, Cl and F were repeatedly analyzed by both methods in three in-house natural glass standards (obsidians from Lipari, Eolian Islands (LIP), Italy; Little Glass Mountain, California (LGM), United States; and Corbetti volcano (CO5), Ethiopia). The results show a slight overestimation of both F and Cl concentrations determined by EPMA compared to pyrohydrolysis. For intercalibration of each EPMA session, the same natural glass samples were used as internal standards. Furthermore, standards and samples were always carbon coated together to avoid analytical differences arising from carbon coat thickness. Measurements of glass compositions may be biased by the presence of undetected microlites within the analyzed volume. Analytical data are, therefore, selected using major element diagrams combining the analyses of glass and mineral compositions. Analyses displaying evidence of a contribution from a mineral phase were discarded. No EPMA analytical routine exists for the other halogens (Br and I).

[18] The H<sub>2</sub>O concentrations of some glasses from the Vesuvius eruption were estimated using EPMA and the “by difference method” [Devine and Gardner, 1995], calibrated on the three in-house natural glass standards and melt inclusions in quartz from Mont Dore volcano (Massif Central, France [Clocchiatti, 1975]). The pre-eruptive H<sub>2</sub>O concentration was estimated from multiphase equilibrium for the Vesuvius eruption, and the results were

similar to those obtained by FTIR [Cioni, 2000]. Other H<sub>2</sub>O concentrations are from the literature.

[19] Due to the high crystallinity or the high vesicularity of some samples that limit the size of the glassy areas, point measurements by EMPA may be impossible. In those cases, volatile concentrations in the groundmass, representing matrix glass plus microlites (the microlite weight fraction is inherited from syn-eruptive degassing and can be measured from SEM image analysis), may be estimated from whole rock composition by correcting for the phenocryst abundance. Estimates of pre-eruptive volatile concentrations may be obtained from melt inclusion analyses. However, in addition to analytical difficulties, possible syn- and post-entrapment evolution (diffusive effects, H<sub>2</sub>O loss, melt inclusion crystallization or immiscibility) may alter the significance of measured volatile concentrations [Lowenstern, 1995; Baker, 2008]. In addition, multistep degassing, which frequently occurs during magma ascent [Druitt et al., 2002; Couch et al., 2003; Balcone-Boissard et al., 2008; Villemant et al., 2008], is generally not recorded in melt inclusions because syn-eruptive crystallization is limited (plinian eruption case), or because multistep degassing does not provide conditions conducive to melt inclusion entrapment. In such cases, pre-eruptive volatile concentrations (i.e., prior to the last degassing stage) cannot be inferred from melt inclusion analyses, which generally only provide minimum values.

### 3. Modeling Halogen Degassing

#### 3.1. Closed Versus Open System Degassing Models

[20] The differences between volcanic eruptive styles are mainly attributed to variations in the degassing regimes [Eichelberger et al., 1986; Jaupart and Allègre, 1991; Eichelberger, 1995; Sparks, 2003; Martel et al., 1998]. Numerous theoretical models based on fluid mechanics have been proposed to account for the variety of eruptive styles [Jaupart and Allègre, 1991; Melnik and Sparks, 1999, 2002; Papale et al., 1998; Voight et al., 1999]. The application of such models to natural systems remains difficult due to the large number of parameters that cannot be measured directly (e.g., viscosity, crystallization kinetics, conduit diameter, magma chamber depth and overpressure, etc.). However, simplified models of magma degassing during eruptions may be calculated using volatile

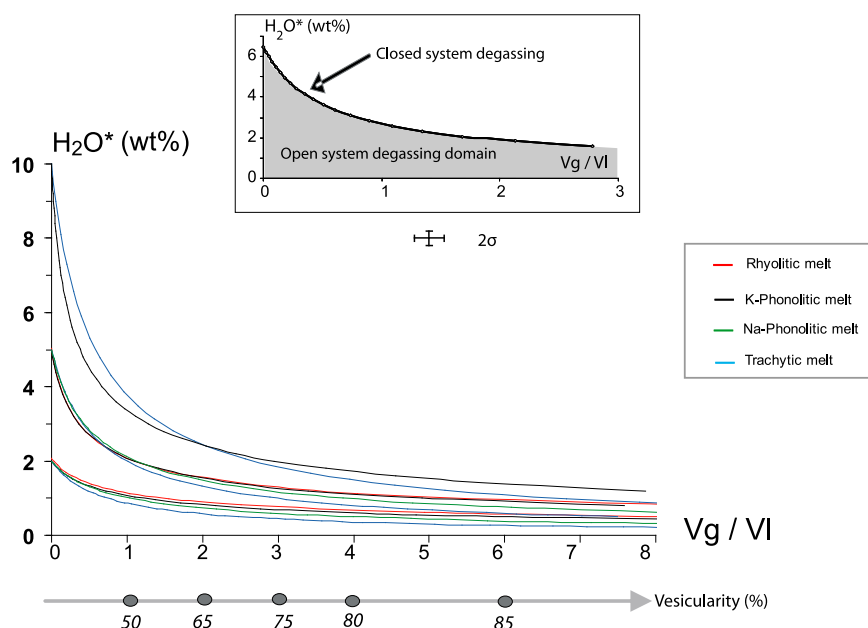


**Figure 1.** Theoretical  $\text{H}_2\text{O}$ -Vesicularity variation during magma degassing. Vesicularity is measured as the volume ratio of gas over melt ( $V_g/V_l$ ; see text for definition). Corresponding vesicularities are given in volume percent, vol%.  $\text{H}_2\text{O}^*$  refers to  $\text{H}_2\text{O}$  concentrations in residual melts. Lines correspond to closed-system evolution for different initial  $\text{H}_2\text{O}$  concentrations (2, 5 and 10 wt%) and melt compositions (rhyolite, Na-phonolite, K-phonolite and trachyte) at the same temperature ( $900^\circ\text{C}$ ). Solubility laws ( $P$  in bars): *Iacono-Marziano et al.* [2007] ( $[\text{H}_2\text{O}] = 0.067 P^{(0.5771)}$ ) for K-phonolite, *Signorelli and Carroll* [2000] ( $[\text{H}_2\text{O}] = 0.0315 P^{(0.7317)}$ ) for Na-phonolite, *Di Matteo et al.* [2004] ( $[\text{H}_2\text{O}] = 0.0114 P^{(0.8663)}$ ) for trachyte and *Liu et al.* [2005] ( $[\text{H}_2\text{O}] = 0.2816 P^{(0.5648)}$ ) for rhyolite. Inset: Solid line: closed-system degassing. Grey: open-system degassing domain, with continuous  $\text{H}_2\text{O}$  loss and vesicle collapse. See text for discussion.

solubility and gas expansion laws, assuming closed- or open-system degassing. Natural systems may be compared to these models using residual volatile concentrations ( $\text{H}_2\text{O}$ ,  $\text{CO}_2$ ,  $\text{SO}_2$ , halogens) and textural characteristics (vesicularity, microcrystallinity) measured in erupted magma fragments [Villemant and Boudon, 1998; Villemant et al., 2003, 2008; H. Balcone-Boissard et al., Textural and geochemical constraints on eruptive style of the 79AD eruption at Vesuvius, submitted to *Bulletin of Volcanology*, 2010]. Because eruptions sample magma quenched at different depths and gas pressures, measurements of vesicularity and volatile concentrations on a series of magma fragments collected from different units of the same eruptive phase allow reconstruction of degassing paths.

[21] Because  $\text{H}_2\text{O}$  is the major volatile species in felsic magmas, modeling degassing paths requires knowledge of the  $\text{H}_2\text{O}$  solubility law in the melt [Burnham, 1975, 1994; Carroll and Blank, 1997; Di Matteo et al., 2004; Zhang, 1999]. First, assuming an initial pre-eruptive  $\text{H}_2\text{O}$  concentration, the closed system degassing path may be theoretically calculated and represented in the  $[\text{H}_2\text{O}]_r$ - $V_g/V_l$  diagram, where  $[\text{H}_2\text{O}]_r$  is the residual

water concentration in glass from a pumice clast and  $V_g/V_l$  is ratio of the volume of gas ( $V_g$ ) to the volume of melt ( $V_l$ ) in the clast. During magma ascent from the  $\text{H}_2\text{O}$  saturation depth,  $\text{H}_2\text{O}$  exsolves with decreasing pressure, bubbles form and expand in response to both the decrease in  $\text{H}_2\text{O}$  solubility and the decrease in pressure (Figure 1) [Villemant and Boudon, 1998, 1999]. In this degassing regime, the residual  $\text{H}_2\text{O}$  concentration rapidly reaches an almost constant value depending on the bulk melt composition and initial  $\text{H}_2\text{O}$  concentration. The closed system degassing model represents the typical model for plinian eruptions [Eichelberger, 1995; Jaupart and Allègre, 1991].

[22] In natural systems, pumice clasts with vesicularities lower than 50% or higher than 80–90% are rarely observed, which limits the range of measured  $V_g/V_l$  values to between approximately 1 and 7. Within that vesicularity range, closed system degassing curves are very similar for identical initial  $\text{H}_2\text{O}$  concentrations in different composition magmas. More precisely, due to the similarity of their  $\text{H}_2\text{O}$  solubility behavior, rhyolites and K-phonolites on one hand, and Na-phonolites and trachytes on the other hand, produce indistinguishable closed sys-



tem degassing curves. Additionally, closed system degassing models are not sensitive, within analytical errors, to temperature variations in the range of 800 to 1000°C (Figure 1).

[23] Alternatively, for highly degassed and highly vesiculated melts, H<sub>2</sub>O exsolution may be reduced or stopped whereas gas expansion continues due only to the pressure decrease (“expansion only evolution,” Figure 1). This may occur if the H<sub>2</sub>O transfer rate from the melt to bubbles is strongly reduced, whereas melt viscosity remains sufficiently low to allow continuous bubble expansion. The reduction of the H<sub>2</sub>O transfer rate may be due, for example, to a large increase of the ascent rate (decompression) relative to H<sub>2</sub>O diffusion or to variations in bulk H<sub>2</sub>O diffusivity related to variations in OH<sup>−</sup> and H<sub>2</sub>O species in the melt [Watson, 1994; Zhang *et al.*, 1991]. Vesicle expansion with no H<sub>2</sub>O depletion in matrix glass has been proposed to occur during a short interval of time after fragmentation, in the volcanic plume [Thomas *et al.*, 1994; Gardner *et al.*, 1996; Kaminski and Jaupart, 1997].

[24] In the open system degassing mode, exsolved gas continuously escapes from the magma column, for instance through conduit walls. This mode results in decreasing vesicularity as volatile concentrations in the melts fall. Because this gas loss leads to a decrease of magma ascent rates, crystallization induced by degassing may be extensive [Burnham, 1979; Hammer *et al.*, 1999; Blundy and Cashman, 2001; Couch *et al.*, 2003; Atlas *et al.*, 2006], as observed in lava dome-forming eruptions, and lower ascent rates and crystallization lead to larger volatile degassing. Both processes (gas escape and degassing-induced crystallization) may be modeled with the Rayleigh distillation law [Villemant and Boudon, 1998; Melnik and Sparks, 1999; Villemant *et al.*, 2003, 2008].

[25] The behavior of minor volatile elements, such as halogens, may be described using H<sub>2</sub>O degassing models and H<sub>2</sub>O vapor/melt partition coefficients [Villemant and Boudon, 1998]. The theoretical evolution of residual halogen concentrations versus V<sub>g</sub>/V<sub>l</sub> display similar features to those for H<sub>2</sub>O and emphasize that halogen extraction is primarily dependent on both the halogen concentrations in pre-eruptive melts (Figure 1) and the amount of extracted H<sub>2</sub>O. H<sub>2</sub>O vapor/melt partition coefficients also vary with melt composition and pressure, which induces second order variations in closed- and open-system degassing models [Villemant *et al.*, 2003; Shinohara, 2009].

## 3.2. Geochemical Parameters Controlling the Behavior of Halogens During the Degassing of Magmas

[26] Differences in degassing efficiency may be related to variations in the fluid/melt partition coefficients of volatiles, to kinetic effects (competition between degassing and crystallization processes and volatile diffusivity) and/or to modifications of magmatic properties such as viscosity (melt viscosity).

### 3.2.1. Solubility and Fluid/Melt Partition Coefficients of Halogens in Felsic Magmas: The Example of Cl

[27] Chlorine discharge by volcanoes into the atmosphere is highly variable, but HCl is always the dominant Cl-bearing gas species [Giggenbach, 1996; Allard *et al.*, 2005; Oppenheimer *et al.*, 2006; Burton *et al.*, 2007]. By contrast, Cl speciation in high pressure H<sub>2</sub>O-rich fluids (i.e., P > 100 MPa) is dominated by chloride salts, such as NaCl and KCl as evidenced by fluid inclusion studies and experiments [Burnham, 1975; Anderko and Pitzer, 1993a; Lowenstern, 1994; Liebscher, 2007; Driesner and Heinrich, 2007]. Thus, Cl extraction from melts is controlled by degassing of H<sub>2</sub>O vapor, and Cl distribution and speciation between silicate melts and H<sub>2</sub>O-rich fluids display large pressure dependencies [Sourirajan and Kennedy, 1962; Shinohara, 1994, 2009; Candela and Piccoli, 1995]. For high Cl concentrations and pressures lower than ~200 MPa, fluid immiscibility generally occurs, generating a Cl-poor H<sub>2</sub>O vapor and a dense Cl-rich hydrous fluid. Numerous studies have investigated Cl distribution in various silicate melt compositions and experimentally determined Cl fluid/melt partition coefficients ( $K_{\text{Cl}}^{\text{f/m}}$ ) [Kilinc and Burnham, 1972; Webster and Holloway, 1988; Shinohara *et al.*, 1989; Métrich and Rutherford, 1992; Webster, 1992a; Kravchuk and Keppler, 1994; Shinohara, 1994; Candela and Piccoli, 1995; Webster, 1997; Webster and Rebbert, 1998; Signorelli and Carroll, 2000; Carroll, 2005; Chevychelov *et al.*, 2008; Alletti *et al.*, 2009]. These experimental results indicate that  $K_{\text{Cl}}^{\text{f/m}}$  depends on pressure and temperature, melt composition (in particular the Na<sup>+</sup>/K/Al ratio) and H<sub>2</sub>O and Cl melt concentrations.  $K_{\text{Cl}}^{\text{f/m}}$  values increase with decreasing temperature, decreasing/increasing pressure and increasing Cl concentrations in the melt. Temperature effects are generally considered negligible because temperature variations during the studied degassing processes are

low and the temperature dependence of  $K_{\text{Cl}}^{\text{f/m}}$  is low. The dependence of  $K_{\text{Cl}}^{\text{f/m}}$  with pressure is significant but no experimental data for felsic magmas exist for  $P < 50$  MPa, where HCl is the dominant species (for basalts, see *Alletti et al.* [2009]).  $K_{\text{Cl}}^{\text{f/m}}$  values increase with increasing silica activity or decreasing Mg, Ca or Fe concentrations; they are maximized for subaluminous melts [ $\text{Na}^+\text{K}/\text{Al} \sim 1$ ] and decrease as melts become more aluminous or peralkaline. Experimental data indicate that  $K_{\text{Cl}}^{\text{f/m}}$  values are higher for rhyolitic melts than for alkaline felsic melts. During magma ascent, the large extent of degassing-induced crystallization modifies melt compositions and tends to increase  $K_{\text{Cl}}^{\text{f/m}}$  in rhyolitic melts as the Si concentration increases and Mg, Ca and Fe decrease, and as the  $(\text{Na}^+\text{K})/\text{Al}$  ratio tends toward 1 [*Villemant et al.*, 2003]. Modeling of degassing during open system conditions including melt crystallization shows that the behavior of  $\text{H}_2\text{O}$  and halogens are consistently reproduced using experimental equilibrium partition coefficients and their variations with melt composition [*Villemant et al.*, 2003, 2008]. Bulk melt composition, melt Cl concentration and pressure are probably the most influential parameters on  $K_{\text{Cl}}^{\text{f/m}}$  in the studied systems.

### 3.2.2. Kinetic Effects: Role of Diffusivities and Viscosities

[28] Volatile diffusivity in melts may significantly affect their degassing efficiency especially for rapid magma ascent rates during plinian eruptions [*Alletti et al.*, 2007; *Gardner et al.*, 2006]. Volatile transfer from melt to vesicles depends both on the equilibrium  $K_{\text{Cl}}^{\text{f/m}}$  values and as well as on diffusion coefficients, chemical gradients, the thickness of bubble walls and time. Cl diffusivities in felsic melts are one order of magnitude slower than  $\text{H}_2\text{O}$  diffusivities [*Bai and Koster van Groos*, 1994]. Bubble growth models in a semi-infinite medium show that for bubble growth rates higher than  $10^{-8} \text{ m}^2 \text{ s}^{-1}$ , which prevail during plinian eruptions, and for large  $K_{\text{Cl}}^{\text{f/m}}$  values, departures away from equilibrium compositions may be significant for Cl [*Balcone-Boissard et al.*, 2008]. However, during magma ascent, vesicles nucleate and expand rapidly so that the distance between bubbles is strongly reduced for large vesicularities. The mean diffusive path length of volatiles in the melt becomes rapidly smaller than the bubble wall thickness and diffusion has a negligible effect on the gas composition in the bubbles. It is unlikely that diffusion has a sufficiently limiting effect to explain the observation that all the investigated felsic

magmas from plinian eruptions display effective  $K_{\text{Cl}}^{\text{f/m}}$  values lower than equilibrium values.  $K_{\text{Cl}}^{\text{f/m}}$  values required to model Cl evolution during lava dome-forming eruptions are close to equilibrium values. This observation indicates that diffusion is probably not a limiting factor. Ascent and degassing rates are much lower than during plinian eruptions favoring equilibrium processes. Moreover, the degassing-induced crystallization of melts significantly increases the gradient in volatile concentrations between melt and vesicles, which enhances  $\text{H}_2\text{O}$  and halogen transport from melt to vesicles.

[29] Melt viscosity is strongly dependent on variations of temperature, dissolved  $\text{H}_2\text{O}$  concentrations and bulk melt composition, while pressure dependence is insignificant below 2 GPa [*Dingwell et al.*, 1996].  $\text{H}_2\text{O}$  degassing significantly increases magma viscosity by increasing the degree of silicate melt polymerization and by inducing melt crystallization [*Atlas et al.*, 2006; *Giordano et al.*, 2008].

## 4. Results

[30] Major element compositions of bulk rocks and groundmass (assumed to be equivalent to residual melts) for each eruption are given in Table 1. Calculated crystallinity and microcrystallinity estimates are reported in Table 2a. Measured  $\text{H}_2\text{O}$  and halogen composition ranges of groundmass are given in Table 2b. When available, estimates of “initial” volatile concentrations from melt inclusion analyses are also reported.

### 4.1. Vesicularity, Crystallinity and Microcrystallinity

[31] We collected at least 100 pumice clasts in each eruptive unit, and sieved them (with a sieve of 16 mm in diameter) to select fragments large enough to perform all analyses on the same clast. Each pumice clast was washed and sawed into three parts: the first part was used for density measurements, the second part was powdered for bulk chemical analyses, and the third part was dedicated to thin section preparation for textural characterization (SEM) and chemical microanalysis (EPMA). The analyzed volcanic clasts were selected on the basis of their density distribution. At least three pumice clasts were selected, one near the median density and one each at the low and high density tails. They represent a large range of degassing regimes and degrees, characteristic of the degassing processes involved in the different

**Table 2a.** Range of Halogen and H<sub>2</sub>O Concentrations in the Groundmass and the Crystallinities of Clasts From the Different Eruptions<sup>a</sup>

	Vesuvius, 79AD WP	Fogo, Fogo A	Montagne Pelée, P1		Santa Maria-Santiaguito, 1902–1929	
	Plinian Clasts	Plinian Clasts	Lava Dome Fragment	Plinian Clasts	Lava Dome Fragment	Plinian Clasts
F (ppm)	2300–5500	700–4200	20–300	150–300	100–300	200–350
Cl (ppm)	3600–6000	1000–6500	30–750	900–1500	100–650	800–1300
Br (ppm)	2–9	5–19	0–3	3–5	0–2	1–3
I (ppb)	50–200	45–350	nd	50–100	10–15	10–45
H <sub>2</sub> O (wt%)	0.9–1.4	0.7–2.4	0–1.2	1.4–2	0–0.9	1.2–1.9
Crystallinity (wt%)	8	5–15	30–40	25–30	30–36	20–30
Microcrystallinity (wt%)	30	ε	>80	ε	>80	ε

<sup>a</sup>H<sub>2</sub>O and halogen concentrations: whole rock measurements corrected for phenocryst content. Crystallinity: weight fraction of phenocrysts in bulk rocks estimated from mass balance calculations except for Fogo A, where image analysis was used. Microcrystallinity: weight fraction of microlites in the groundmass, estimated from SEM images, except for the Vesuvius eruption. For the Vesuvius white pumice the microcrystallinity was estimated from F and Cl concentrations assuming no degassing and incompatible element behavior; these estimates are consistent with literature data (SEM image analysis [Gurioli et al., 2005]). ε: negligible amounts.

eruptions. In eruptions that had both explosive and effusive phases textural and chemical characteristics of both pumice clasts and lava-dome fragments were studied.

[32] In large phonolitic and trachytic plinian eruptions, the vesicularity distribution is unimodal, centered around 80%, with a low dispersion. The calc-alkaline plinian eruptions display similar vesicularity ranges and distributions. Lava-dome fragments have significantly lower vesicularities than pumice clasts. All studied plinian sequences are characterized by highly vesicular pumice clasts, irrespective of chemical composition (rhyolite, trachyte or phonolite). Pumice clasts show large, spherical bubbles (from a few microns to around one hundred microns in diameter) with thin glassy septae ( $\leq 5\text{ mm}$  thick), which are evidence supporting the lack of significant gas loss and melt crystallization during magma ascent and degassing. Conversely, vesicles in lava-dome fragments display a large variation in size and shape, with complex, contorted bubbles, evidence of vesicle coalescence and flattening that occasionally create degassing channels, indicating that gas was able to escape from the magma column. The coalesced bubbles may reach several hundreds of micro-

meters in length, with bubble wall thicknesses larger than 100  $\mu\text{m}$ . The phenocryst concentrations in calc-alkaline magmas (rhyolitic melt) are high (>25 wt%) compared to the other melts; trachytic and phonolitic melts display low phenocryst concentrations (<10 wt%). Plinian eruptive products contain glassy matrices with no or low (<30 wt%) microlite concentrations, indicating that melt is in a metastable state, as a result of the high magma ascent velocity that prevented the melt from crystallizing by kinetic limitations until the point of fragmentation and quenching. However, the matrices of lava-dome fragments are highly microcrystalline (up to 100% in some cases), indicating that degassing and crystallization processes occurred at equilibrium.

## 4.2. Relative Behavior of Halogens During Felsic Magma Differentiation and Degassing

[33] Both pre-eruptive melts (preserved in melt inclusion) and post-eruptive melts (residual glass in groundmass) of trachytic and phonolitic magmas contain higher concentrations of halogens than rhyolitic melts (Tables 2a and 2b). Cl, Br and I display single correlations (within analytical errors)

**Table 2b.** Volatile Concentrations in Melt Inclusions<sup>a</sup>

	Vesuvius, 79AD WP	Fogo, Fogo A	Montagne Pelée, P1		Santa Maria-Santiaguito, 1902–1929	
	Plinian Clasts	Plinian Clasts	Lava Dome Fragment	Plinian Clasts	Lava Dome Fragment	Plinian Clasts
F (ppm)	2000–5000	500–4500	n.d.	150–300	n.d.	100–300
Cl (ppm)	5300	1300–7500	n.d.	1400–2100	n.d.	700–1600
H <sub>2</sub> O (wt%)	5 (1)	6.5 (2)	n.d.	5.5 (3)	n.d.	5–7 (3)

<sup>a</sup>F and Cl concentrations: EPMA measurements. H<sub>2</sub>O concentrations: (1) estimated from multiphase equilibrium of a Cl-rich H<sub>2</sub>O vapor [Balcone-Boissard et al., 2008]; (2) literature data [Wolff and Storey, 1983]; (3) EPMA using the “by-difference” method. n.d.: not determined.

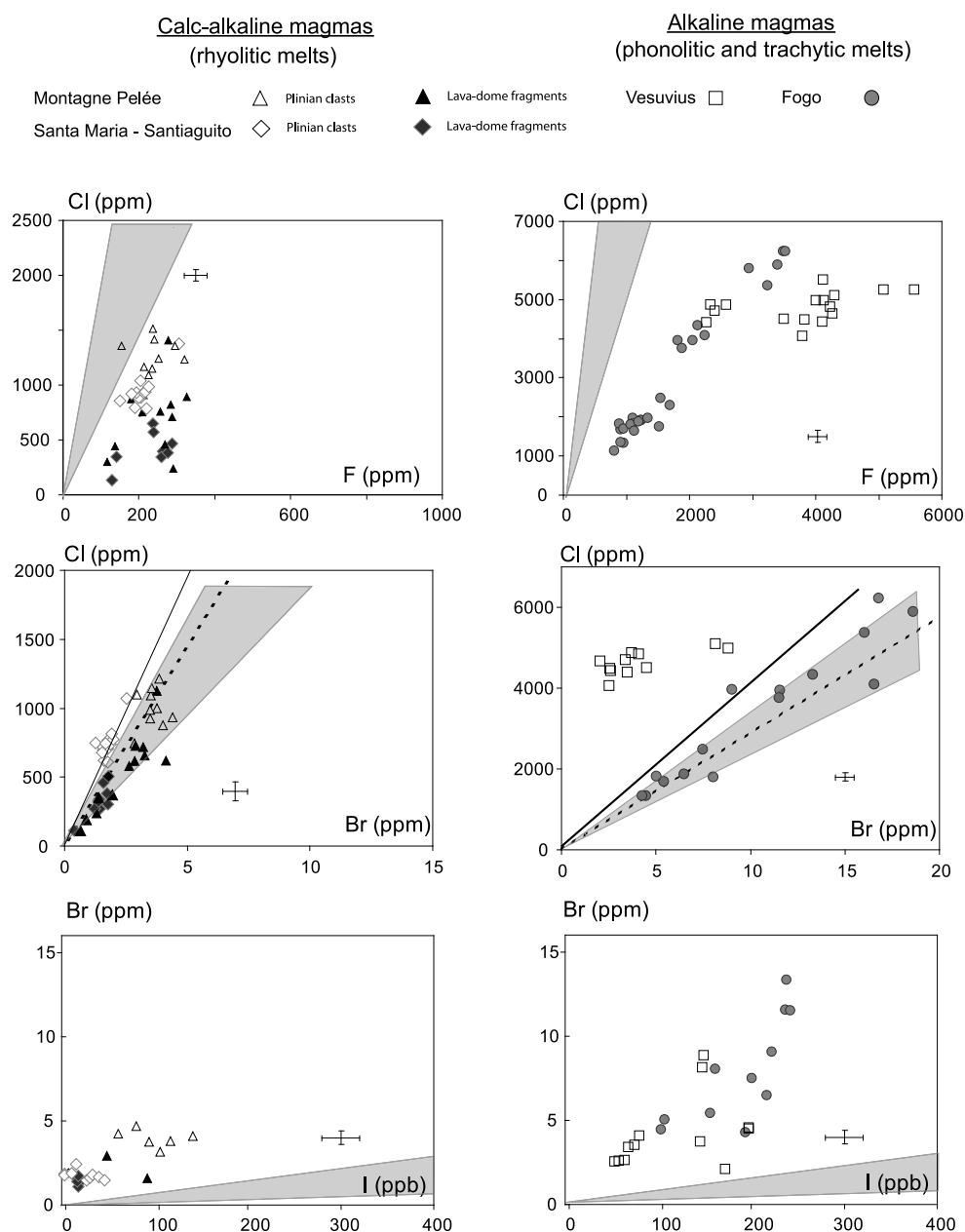


**Figure 2.** Halogen composition of groundmass from alkaline and calc-alkaline magmas (trachytic, phonolitic and rhyolitic melts). Compositions are obtained from bulk rock analyses corrected for phenocryst concentrations. Chemical ratios (Cl/F, Cl/Br, Br/I) of some reference materials are also plotted: chondrites (gray domain), basalts (solid line) and seawater (dashed line) (literature data, see Table 3). Compositional ranges are reported in Table 2a. Each alkaline magmatic system (Vesuvius and Fogo A, on the right) is represented by one symbol corresponding to plinian activity. Each calc-alkaline system (Montagne Pelée and Santa Maria–Santiaguito, on the left) is represented by two symbols corresponding to plinian (open symbols) and lava-dome forming eruptions (solid symbols).

for each studied eruption, irrespective of variations in initial melt compositions or degassing regime (Figure 2). However, due to the low precision of the I measurements, the constancy of the Br/I ratio is puzzling and should be confirmed by more accurate and precise iodine measurements, which requires further improvements in analytical tech-

niques. [Michel and Villemant, 2003; Chai and Muramatsu, 2007; Balcone-Boissard et al., 2009]. Relative to other halogens, the behavior of F is variable and mainly depends on magma composition (Figure 2). In trachytic melts, F is always linearly correlated to Cl. In the phonolitic melt of Vesuvius, F and Cl are not correlated because of



**Table 3.** Ranges of Cl/F, Cl/Br and Br/I Ratios for the Studied Eruptions: Comparison With Basalts, Seawater and Meteorites<sup>a</sup>

Volcano	Eruption	Sample Type	Cl/F	Cl/Br	Br/I
Alkaline magmas					
Vesuvius	79 AD	WP	1–2	500–1500	25–50
Fogo	Fogo A	pumice	1.5–2	250–400	30–50
Calc-alkaline magmas					
Montagne Pelée	P1	lava dome fragments	2.5–5	200–300	nd
		pumice	3.5–6	250–400	30–100
Santa Maria/Santiagouito	1902–1929	lava dome fragments	1.4–1.6	200–300	100–200
		pumice	0.5–4	500–600	30–200
Soufrière Hills (Montserrat)	1996–1997	lava dome fragments	4–8	100–400	50–150
		pumice	8–140	150–450	100–200
Seawater			14900	288	1250
Meteorites			6–15	200–400	0.1–0.5
Basalts		MORB		430 ± 130	

<sup>a</sup>Range: minimum and maximum halogen ratios of individual clasts. Meteorites: *Dreibus et al.* [2004]. Basalt: *Schilling et al.* [1980].

small variations in Cl concentrations. In calc-alkaline magmas (rhyolitic melts), the F concentration in the groundmass remains almost constant within a relatively low and narrow range (100–300 ppm), in contrast to other halogens, whose concentrations vary significantly with degassing (as a result of H<sub>2</sub>O loss).

#### 4.2.1. Cl/F Ratio

[34] In alkaline magmas the Cl/F ratio of pumice clasts is constant for a given eruption and varies within a narrow range for all studied systems (Cl/F = [1–2]; except for Vesuvius). In calc-alkaline systems (rhyolitic melts) the Cl/F range of lava-dome fragments and pumice clasts is larger ([2–8]; Figure 2). The Cl/F ratio in pumice is always twice as high as in lava-dome fragments (Figure 2). The Cl/F ratios of the investigated magmas are considerably lower than the Cl/F ratio of seawater (~15000), which is characterized by an extreme depletion in F, but are similar to chondrites (6–15 [Goles and Greenland, 1966; Dreibus et al., 1979, 2004]).

#### 4.2.2. Cl/Br Ratio

[35] The Cl/Br ratio ranges between 170 and 1000, with no apparent systematic behavior between different volcanoes and melt compositions. The Cl/Br ratio of all studied magmatic systems covers the whole range of Cl/Br ratios observed for chondrites (200–400), basalts (430 ± 130 in MORB [Schilling et al., 1980; Jambon et al., 1995]) and seawater (300). Such large variations in magma compositions at small spatial or temporal scales are also observed for the Santa Maria-Santiagouito samples, for which the Cl/Br ratio of the 1902 plinian products is ~500 whereas the lava dome-forming

fragments from the same time period have a Cl/Br ratio of ~300 (Table 3). The magma source of the 1902 eruption could have been depleted in Br relative to Cl. Small scale heterogeneities in Cl/Br ratios of magma sources are of the same magnitude for all calc-alkaline series (Guatemala and Antilles). The large plinian eruption of Fogo A also displays a seawater-like Cl/Br ratio, whereas Vesuvius magmas have a high Cl/Br ratio of ~850 ± 200.

#### 4.2.3. Br/I Ratio

[36] The Br/I ratio is apparently homogeneous (~45) in the pumices of Fogo A, Vesuvius and Montagne Pelée, whereas Br/I is higher (~90) in clasts from the Santa Maria-Santiagouito eruption. The Br/I ratio for lava-dome fragments is high (~110) in clasts from the Santa Maria-Santiagouito eruption. The Br/I ratio measured in volcanic rocks is apparently lower than the mean ratio of chondrites [Goles and Greenland, 1966; Dreibus et al., 2004], but, as indicated above, this result has to be confirmed by more accurate analyses.

### 5. Discussion: The Relative Behavior of Halogens

[37] Correlations between volatile concentrations of the different clasts from the same eruptive sequence may be interpreted in terms of their relative behavior during shallow degassing and/or magma differentiation. A linear correlation through the origin indicates that the volatile species display similar behavior, i.e., similar crystal/melt and vapor/melt partition coefficients. If the residual concentrations of two halogens in volcanic clasts are correlated through the origin, their ratio is constant and characteristic of the shallow magma reservoir.



[38] The measurements show a large range of Cl/F ratios in calc-alkaline magmas. This range is related to the different behavior of F and of Cl during H<sub>2</sub>O degassing that lead to large variations in Cl, Br, and I concentrations, whereas F concentrations remain almost constant in different clasts. Conversely Cl/Br/I ratios are always preserved during magma degassing and differentiation, at least in differentiated magmas (acid andesites, trachytes and phonolites). As a consequence, the halogen (except F) ratios for one magmatic system may be estimated from the measurement in any erupted product and linked to the halogen concentration characteristics of the shallow magma reservoir. This result is likely valid for basaltic magmas and their differentiation products because most mineral phases involved in basaltic petrogenesis do not fractionate halogens. However, halogen-bearing minerals (amphiboles, micas, apatites, etc.) may fractionate halogens and thus modify halogen ratios in magmas. These variations may be generally limited because they depend on both the halogen concentration in minerals, the mineral weight fraction, and the mineral halogen ratio (see for example the case of amphiboles in Soufrière Hills, Montserrat [Villemant *et al.*, 2008]). In addition, calc-alkaline magmas display variable ratios from one volcano to another, possibly due to modification of the Cl/Br/I ratios by fluid transfer during mantle partial melting, contamination or fluid recycling in subduction zones [Wallace, 2005]. The large variations in halogen ratios between meteorites and magmas reflect fractionation occurring during early differentiation of Earth. This distribution reflects halogen incompatibility during partial melting. Little is known about the concentrations of halogens in the solid earth reservoirs and about the main factor controlling the behavior of halogens during other processes such as crystallization and degassing, and their role in subduction zones to discuss about halogen recycling [Kent *et al.*, 2002; Straub and Layne, 2003; Wallace, 2005; Aiuppa *et al.*, 2009].

## 5.1. Behavior of Halogens During Alkaline Magma Differentiation and Degassing

### 5.1.1. Incompatible and Non-volatile Behavior of Halogens: The Fogo A Eruption

[39] Halogen concentrations in pumice clasts emitted during the plinian phase of the Fogo A eruption vary through a large range but display constant F/Cl/Br/I ratios (Figures 2 and 3). The halogen concentrations are highly homogeneous within a given eruptive unit and strongly decrease

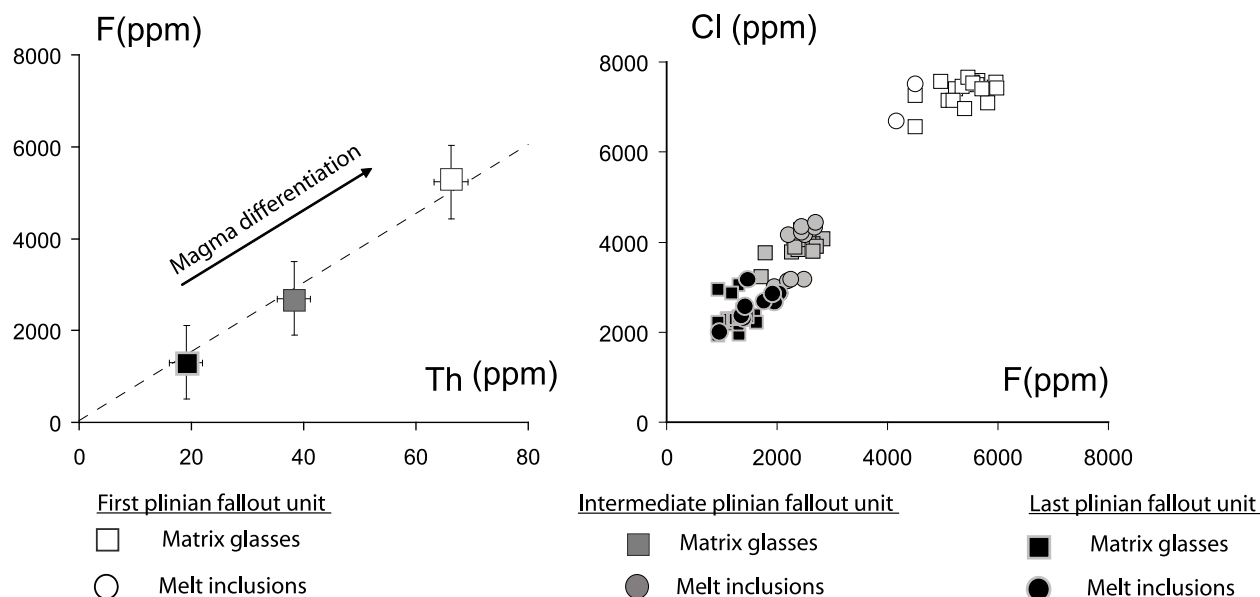
from the first to the last plinian fallout. F remains linearly correlated to Th from the first to the last plinian fallout indicating that F behaves incompatibly (Figure 3a). Correlations through the origin (Figures 2 and 3) between all halogens from all the plinian fallout units demonstrate that during magma differentiation halogens behave as incompatible elements and no volatile-rich mineral phase was able to fractionate halogens crystallizes in sufficient amounts to significantly modify their relative abundances. This halogen zonation is acquired by magmatic differentiation at depth, as exemplified by melt chemistry [Widom *et al.*, 1992; Watanabe *et al.*, 2005; Snyder *et al.*, 2007]. Melt inclusions and the corresponding matrix glass have similar F and Cl concentrations (Figure 3a) in all eruptive units. Residual H<sub>2</sub>O concentrations in all pumice clasts are low (~0.5–2.5 wt% H<sub>2</sub>O; groundmass concentration; Figure 5) compared to the initial H<sub>2</sub>O concentration of 6.5 wt% [Wolff and Storey, 1983]: H<sub>2</sub>O is extracted during magma ascent which controls the plinian eruptive regime. On the contrary, halogens are not significantly extracted from the melt during H<sub>2</sub>O degassing. In addition, halogens are not significantly fractionated relative to each other, at both the deep magma differentiation stage and the shallow degassing stage, which means that the halogen composition of erupted fragments directly reflects that of the pre-eruptive magma.

### 5.1.2. Pre-eruptive Fractionation and Syn-eruptive Non-volatile Behavior of Halogens: The Vesuvius Eruption

[40] F and Cl concentrations measured in the white pumice clasts of the Vesuvius eruption are higher in the matrix glass than in melt inclusions (Figure 3b). Contrary to the Fogo A eruption, syneruptive crystallization is significant during the white pumice plinian phase (Balcone-Boissard *et al.*, submitted manuscript, 2010). The close correspondence between microcrystallinity estimates (~25–35%, image analysis [Gurioli *et al.*, 2005]) and F and Cl enrichment factors between melt inclusions and matrix glasses (~20–40%, Figure 3b) also suggests that halogens behave as incompatible elements during syn-eruptive melt crystallization and are not significantly affected by degassing processes.

[41] The behavior of halogens in the reservoir prior the Vesuvius eruption is complex (Figure 3b). Balcone-Boissard *et al.* [2008] have shown that prior to eruption parts of the magma, though displaying significant variations in differentiation degree have almost constant Cl concentrations.

### a/ Fogo A



### b/ Vesuvius

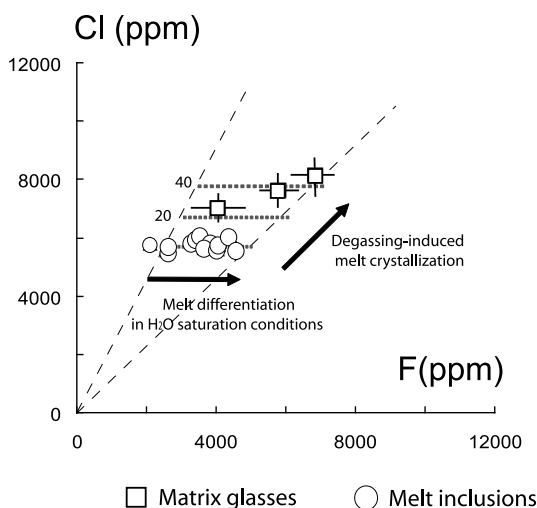


**Figure 3.** F and Cl concentrations in melt inclusions and matrix glasses of the Vesuvius (phonolite) and the Fogo A (trachyte) plinian eruptions. (a) F, Cl and Th concentrations in matrix glass and melt inclusions in Fogo A. F and Cl concentrations in matrix glass and melt inclusions are measured by EPMA (first plinian fallout: 22 values; last plinian fallout: 17 values). Th concentrations are obtained by ICP-MS on separated glass (first plinian fallout: 3 values; last plinian fallout: 4 values). Mean F and Th in the three eruptive units display a clear linear correlation through the origin indicating that F is an incompatible element. F and Cl concentrations of melt inclusions (circles) and matrix glasses (squares) are identical in pumice clasts irrespective of the eruptive unit. Open symbol: first plinian fallout eruptive unit. Grey symbol: intermediate plinian fallout eruptive unit. Black symbol: last plinian fallout eruptive unit. (b) F and Cl contents in matrix glass and melt inclusions of white pumice clasts of Vesuvius. Squares: mean values of at least 10 analyses of matrix glasses from three fallout units [Balcone-Boissard *et al.*, 2008]. Circles: individual measurements of halogen concentrations in melt inclusions from feldspars. F concentrations in melt inclusions vary at constant Cl concentrations that correspond to melt differentiation in H<sub>2</sub>O-saturation conditions. Differences in Cl and F concentrations between melt inclusions and matrix glass result from syn-eruptive crystallization (degassing-induced melt crystallization). Dashed horizontal lines refer to the calculated effects of different degrees of syn-eruptive melt crystallization (in wt%). The analytical uncertainty is smaller than the symbol size.

This Cl buffering effect is interpreted as the result of aqueous fluid + brine saturation of the melt. At a given T, P and melt composition, part of the pre-eruptive silicate melt is in equilibrium with two immiscible fluid phases (a H<sub>2</sub>O-rich vapor and a Cl-rich brine). Equilibrium between silicate melt and subcritical NaCl-H<sub>2</sub>O fluids, at a given temperature and pressure, fixes the Cl concentration in the three coexisting phases [Lowenstern, 1994; Signorelli and Capaccioni, 1999; Signorelli and Carroll, 2000]. At these conditions, the knowledge of the Cl melt concentration allows estimation of pre-eruptive conditions (H<sub>2</sub>O concentration and pressure), using Cl and H<sub>2</sub>O solubility laws [Balcone-Boissard et al., 2008]. This particular process occurs in Cl-rich phonolitic melts that reached H<sub>2</sub>O saturation at relatively low pressure (~180 MPa). At such pressures, H<sub>2</sub>O exsolution strongly depletes the melt in Cl. This is not the case if the melt with similar composition is H<sub>2</sub>O undersaturated. The relative behavior of Cl and Br in the white pumice melts suggest that Br may also be affected by such fluid immiscibility at H<sub>2</sub>O saturation. Contrary to other halogens, F displays no influence of H<sub>2</sub>O saturation.

### 5.1.3. Summary of Halogen Behavior in Alkaline Magmas

[42] The results for trachytic and phonolitic melts show that during plinian eruptions involving alkaline magmas, halogens cannot be significantly extracted from the melts by rapid H<sub>2</sub>O degassing. The Cl concentrations in residual glasses are not related to the large variations in H<sub>2</sub>O concentrations. This observation demonstrates that Cl is insensitive to explosive magma degassing. However, if magmas are H<sub>2</sub>O-saturated prior eruption, Cl (and possibly other halogens) may be significantly extracted into the fluid phase before eruption, as exemplified by Vesuvius. In addition, the existence of a buffered Cl concentration is clear evidence of efficient Cl extraction from pre-eruptive melts into a brine coexisting with a hydrous fluid phase at P < 200 MPa. If pre-eruptive H<sub>2</sub>O saturation occurs at P > 200 MPa, only a single H<sub>2</sub>O-rich fluid phase is in equilibrium with melt, and the Cl concentration in melt may freely vary. In this case, the analysis of residual melt compositions cannot provide evidence for H<sub>2</sub>O saturation.

[43] The large range of halogen behavior during H<sub>2</sub>O degassing in alkaline magmas is probably related to kinetic effects. Cl extraction by an exsolving H<sub>2</sub>O-rich fluid is highly efficient at rela-

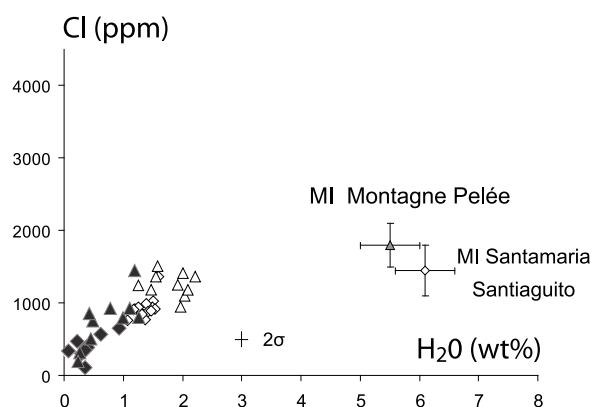
tively high pressures (P < 200 MPa), in pre-eruptive conditions, whereas H<sub>2</sub>O degassing during explosive degassing (plinian eruption) is not efficient at extracting halogens. This suggests that pre-eruptive halogen extraction by a fluid phase in a H<sub>2</sub>O saturated magma occurs at, or at least near, equilibrium, which is not the case for rapid H<sub>2</sub>O extraction characteristic of plinian eruption. However,  $K_{Cl}^{f/m}$  values are highly pressure dependent and, as indicated by the few available experimental data at low pressure and theoretical considerations [see, e.g., Shinohara, 1994, 2009; Candela and Piccoli, 1995; Alletti et al., 2009],  $K_{Cl}^{f/m}$  values may decrease with decreasing pressure. The above results could be indicative of a very rapid decrease of effective  $K_{Cl}^{f/m}$  values down to 0 with decreasing pressure. This rapid variation in Cl solubility in silicate melts in equilibrium with a H<sub>2</sub>O-rich fluid is likely related to the pressure dependence of Cl speciation and to Na<sup>+</sup>, K<sup>+</sup> and H<sup>+</sup> exchange reactions between fluid and melt.

[44] During plinian eruptions of alkaline magmas, the halogen concentrations of gas plumes might be very low because halogens are not significantly affected by shallow explosive H<sub>2</sub>O degassing, unless pre-eruptive fluid phases accumulated in the magma chamber are also emitted at the onset of the eruption.

## 5.2. Halogen and H<sub>2</sub>O Degassing During Calc-Alkaline Magma Eruptions

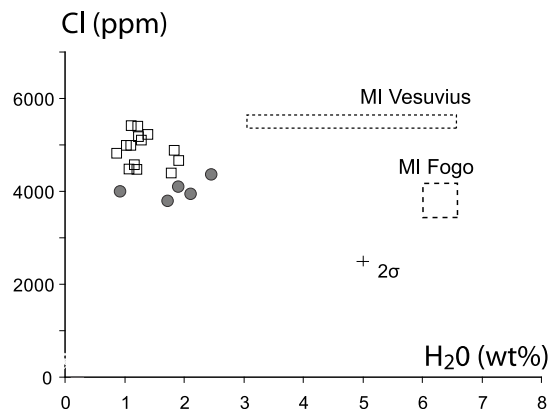
[45] H<sub>2</sub>O is the major volatile phase in rhyolitic melts of calc-alkaline magmas and the H<sub>2</sub>O concentration in erupted clasts varies strongly (Figure 4). H<sub>2</sub>O degassing of rhyolitic melts modifies their Cl, Br and I concentrations (Figure 4; but not F). The pumice clasts and lava-dome fragments emitted during the same eruption (Montagne Pelée or Santa Maria-Santiaguito), involve the same initial melt composition, notably the same initial volatile concentrations. Conversely, the textural characteristics (Table 2a) and the residual volatile concentrations (H<sub>2</sub>O, Cl, Br and I) of the two types of clasts strongly differ. The textural differences reveal different degassing modes. Volatile concentrations in matrix glass or in groundmass of both lava-dome fragments and pumice clasts of the same eruption define continuous trends (Figure 2) with systematically lower values in lava-dome fragments compared to pumice clasts. Degassing is much more efficient in lava dome-forming eruptions than in plinian eruptions, but both degassing regimes follow the same initial degassing steps. Thus, during

(a) Calc-alkaline magmas (rhyolitic melts)



Montagne Pelée    △ Pumice clasts    ▲ Lava-dome fragments  
Santamaria        ◇ Pumice clasts    ◆ Lava-dome fragments  
Santiaguito

(b) Alkaline magmas (phonolitic and trachytic melts)



Vesuvius        □ Pumice clasts  
Fogo            ● Pumice clasts

**Figure 4.** Cl and H<sub>2</sub>O compositions of the groundmass in trachytes, phonolites and rhyolitic melts. For rhyolitic melts (andesite bulk rocks) the mean composition of melt inclusions is reported and the pumice clasts (open symbols) and lava-dome fragments (filled symbols) are identified. For phonolitic and trachytic melts, composition domains of melt inclusions are reported. For Fogo A data are from *Wolff and Storey* [1983].

rhyolitic melt degassing, Cl, Br and I are extracted in the H<sub>2</sub>O vapor phase but the extraction efficiency is strongly dependent upon the degassing regime.

[46] Because of the complex relative behavior of Cl and H<sub>2</sub>O, the apparent Cl/H<sub>2</sub>O ratios measured in volcanic clasts are not conservative parameters (Figure 4). The wide range of Cl/H<sub>2</sub>O ratios may be interpreted as the consequence of strong fractionation between Cl and H<sub>2</sub>O [Wallace, 2005]. In subduction zones many processes may involve Cl/H<sub>2</sub>O fractionation, such as the devolatilization of the slab or the migration of slab-derived fluids through the mantle wedge [Wallace, 2005; Kent *et al.*, 2002]. Melt inclusion compositions are used as best estimates of pre-eruptive melt compositions and the degassing steps leading to plinian eruptions are characterized by large H<sub>2</sub>O losses (by a factor ~3), but a small depletion of Cl (<20%). On the contrary, lava dome-forming eruptions produce more completely degassed magmas, largely depleted in both H<sub>2</sub>O and Cl (Figure 4).

### 5.3. Influence of the Eruptive Style on the Behavior of Halogens

#### 5.3.1. Lava Dome-Forming Eruptions

[47] During lava dome-forming eruptions, here exemplified by calc-alkaline magmas (rhyolitic

melts), both H<sub>2</sub>O and halogen degassing are significant. The compositions of the lava-dome fragments systematically plot in the open system degassing domain (Figure 5). Microlite-rich groundmass, irregular and flattened vesicles and low residual gas concentrations are common features of lava-dome fragments and characteristic of open system degassing. Gas escape from the ascending magma, favored by vesicle connection and collapse, reduces the magma ascent rate and allows melt crystallization in response to H<sub>2</sub>O degassing, which in turn reduces the ascent rate by increasing magma viscosity. H<sub>2</sub>O-vapor/silicate melt partition coefficients of halogens are greater than 1 (except for F) and vary over a large range. Because of the low ascent rate, H<sub>2</sub>O degassing is close to equilibrium during lava dome-forming eruptions and induces two opposite effects on halogen concentrations in matrix glass: depletion (except for F) due to H<sub>2</sub>O vapor exsolution and enrichment due to degassing-induced crystallization. Thus, during degassing-induced melt crystallization the incompatible behavior of halogens competes with degassing effects. The net effect depends directly on the ratio between crystallization and degassing rates, which leads to significant variations of the apparent  $K_{Cl}^{f/m}$  values [Villemant *et al.*, 2008]. The efficient extraction of both H<sub>2</sub>O and halogens (except F) during lava dome-forming

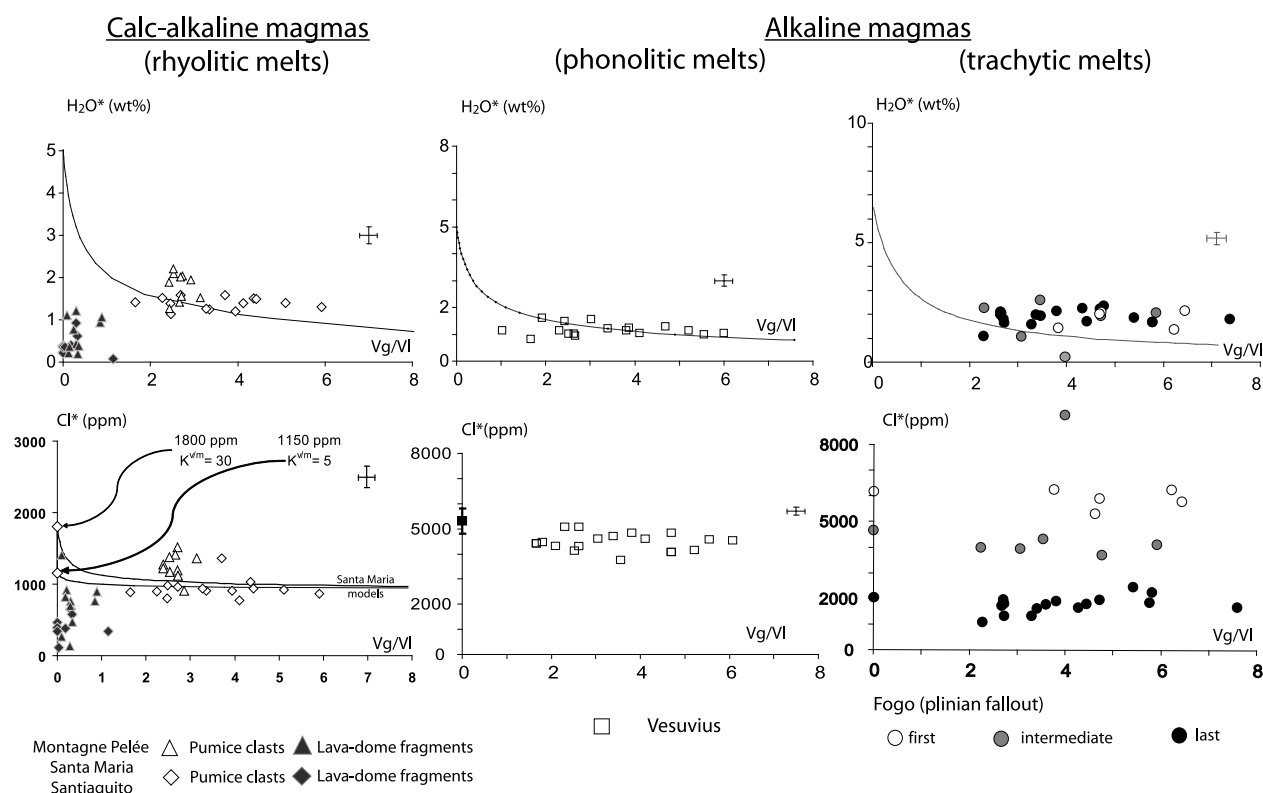


**Figure 5.** Evolution of  $\text{H}_2\text{O}$  and Cl concentrations as a function of vesicularity ( $V_g/V_l$ ).  $\text{H}_2\text{O}$  versus  $V_g/V_l$ : lines correspond to closed-system degassing models for different initial melt compositions (5 wt%  $\text{H}_2\text{O}$  for calc-alkaline magmas and 5 and 6.5 wt%  $\text{H}_2\text{O}$  for alkaline magmas). Cl versus  $V_g/V_l$ : pre-eruptive Cl concentrations are estimated from melt inclusion measurements (mean values) and represented with a  $V_g/V_l = 0$ . For calc-alkaline magmas, lines refer to closed-system degassing models with different initial Cl concentrations (1800 and 1150 ppm, corresponding to the range of Cl concentrations measured in melt inclusions) and  $K_{\text{Cl}}^{v/m}$  values ( $K_{\text{Cl}}^{v/m} = 30$  and 5), which best fit the Santa Maria - Santiaguito clast compositions (Santa Maria models). For alkaline magmas, the range of Cl compositions in melt inclusions is reported ( $V_g/V_l = 0$ ).

eruptions is contrary to what is observed for plinian eruptions (Figure 5). In addition, the large extent of degassing-induced crystallization modifies melt compositions and tends to increase  $K_{\text{Cl}}^{f/m}$  in rhyolitic melts as it increases Si concentration, decreases Mg, Ca and Fe concentrations and as the  $(\text{Na}^+\text{K})/\text{Al}$  ratio tends to 1. Modeling of degassing during dome-forming eruptions (open system degassing model including melt crystallization) shows that the behavior of  $\text{H}_2\text{O}$  and halogens is consistently reproduced using experimental equilibrium partition coefficients and variations with melt compositional evolution [Villemant *et al.*, 2003, 2008]. No lava dome-forming eruption involving phonolitic or trachytic melt has been studied in this paper, but observations on calc-alkaline lava-dome forming eruptions suggest that halogens could also be efficiently extracted during effusive eruptions involving alkaline magmas.

### 5.3.2. Plinian and Vulcanian Eruptions

[48] The evolution of  $\text{H}_2\text{O}$  and Cl concentrations of groundmass as a function of the vesicularity in volcanic clasts from the different plinian eruptions are compared to theoretical models (Figure 1). The high vesicularity with well developed, spherically shaped vesicles separated by an almost completely glassy matrix characteristic of plinian clasts is consistent with the assumptions of the closed-system degassing model. Both  $\text{H}_2\text{O}$  and Cl concentrations in the groundmass of pumice clasts from the calc-alkaline series are consistent with closed system degassing models based on the estimated initial melt compositions (Table 2b), the  $\text{H}_2\text{O}$  solubility law for rhyolitic melts, and assuming low Cl vapor-melt partition coefficients (typically  $\sim 20$ ). The small differences between the Cl concentrations of melt inclusions and of the pumice clast groundmass highlight the low Cl extraction efficiency during



plinian eruptions. Vesiculated clasts of vulcanian eruptions from the ongoing eruption of Soufrière Hills on Montserrat [Villemant *et al.*, 2008; Humphreys *et al.*, 2009], have significantly lower H<sub>2</sub>O concentrations than pumice clasts of the Montagne Pelée and Santa Maria-Santiaguito. This difference is explained by significantly lower H<sub>2</sub>O concentrations in the melt (~2 wt%) before the onset of the vulcanian activity at Soufrière Hills compared to plinian eruptions in similar geodynamic settings. This low initial H<sub>2</sub>O concentration is the result of the very shallow origin of vulcanian explosions, consistent with geophysical data and models [Clarke *et al.*, 2007; Druitt *et al.*, 2002]. At these conditions vulcanian eruptions at Montserrat are only able to extract small amounts of H<sub>2</sub>O and Cl. Because the initial Cl concentrations at Soufrière Hills are two to three times higher than at Montagne Pelée and Santa Maria-Santiaguito, the residual Cl concentrations of Soufrière Hills vulcanian clasts are much higher than in other calc-alkaline pumice clasts. However, the Cl degassing paths in all of these three calc-alkaline eruptions do not differ.

[49] Comparison of the characteristics (vesicularity and water, F, Cl, Br, and I concentrations) of all plinian clasts demonstrates that the range of vesicularities and residual H<sub>2</sub>O concentrations are similar for all eruptions and magma compositions. Degassing paths in H<sub>2</sub>O-Vg/Vl diagrams are wholly consistent with closed system degassing models for Vesuvius [Balcone-Boissard *et al.*, 2008]. For pumice clasts of Fogo A the closed system degassing model is consistent with H<sub>2</sub>O concentrations and vesicularities only if initial H<sub>2</sub>O concentrations are much larger than the previously estimated value of 6.5 wt% [Wolff and Storey, 1983], as shown in Figure 5), which is unlikely. In addition, the bulk vesicularity of these clasts varies while the residual H<sub>2</sub>O concentration remains approximately constant (~2 wt%; Figures 1 and 5). This may be explained by significant late vesicle expansion without further extraction of H<sub>2</sub>O from erupted melt or by differential migration of bubbles in the ascending magma [Kaminski and Jaupart, 1997].

[50] Finally these results show that extraction of Cl and other halogens by H<sub>2</sub>O degassing in the explosive regime (plinian eruptions) is less efficient for trachytic and phonolitic melts than for rhyolitic melts (Figure 5).

## 6. Conclusions

[51] The comparison of residual volatile concentrations and textures of a series of volcanic

clasts emitted during different eruptive regimes from evolved calc-alkaline and alkaline magmas highlights the following general behavior of halogens during H<sub>2</sub>O degassing:

[52] 1. All halogens display a similar behavior during differentiation and degassing of phonolitic and trachytic melts. On the contrary, in calc-alkaline magmas, where the residual melt is rhyolitic in composition, F is fractionated from other halogens during differentiation and degassing processes, due to its greater stability in rhyolitic melt.

[53] 2. Halogen ratios (except those involving F in rhyolitic melts) are conservative during magma differentiation and degassing. Iodine most probably behaves similarly to Br and Cl in rhyolitic melts, but improvements in the analytical technique to achieve higher precision are required to confirm this point. The ratios of Cl/Br/I measured in erupted clasts are thus characteristic of pre-eruptive melts and likely of the more primitive magmas. Nevertheless, these ratios vary from one volcano to another, indicating that halogen fractionation occurred by fluid transfer or by mantle source heterogeneities inherited from early mantle differentiation and recycling.

[54] 3. In alkaline felsic magmas (phonolites and trachytes) halogen concentrations are almost unaffected by H<sub>2</sub>O degassing in the plinian eruption regime. Conversely, during plinian eruptions involving calc-alkaline magmas (rhyolitic melts), Cl, Br and I are significantly extracted by H<sub>2</sub>O degassing, but less efficiently than predicted by available experimental fluid-melt partition coefficients. The difference between the partitioning determined in this study and that determined experimentally can differ by a factor as high as 5.

[55] 4. Effusive degassing during lava dome-forming eruptions of calc-alkaline magmas is more efficient at extracting halogens and H<sub>2</sub>O than explosive degassing. H<sub>2</sub>O and halogen behavior during lava dome-forming eruptions may be modeled assuming equilibrium degassing (i.e., using equilibrium partition coefficients and taking into account degassing-induced melt crystallization). No information is yet available for halogen degassing in the effusive regime of alkaline felsic magmas. These results suggest that halogens would show similar features to those observed for effusive eruptions of calc-alkaline magmas.

[56] 5. The differences in Cl (and probably Br and I) behavior during effusive and explosive degassing cannot only be explained by kinetic effects. As

observed in deep hydrothermal systems and in volcanic plumes, halogen behavior during magma degassing is most probably controlled by speciation. We suggest that both Cl and H<sub>2</sub>O speciation in felsic melts and in exsolved hydrous fluids, which strongly vary with pressure decrease, represent the main factor controlling Cl behavior during the different degassing regimes. The behavior of halogens during explosive degassing is not consistent with experimental data. These differences likely reflect the complex chemical and structural modifications of both melts and hydrous fluids involved during pressure variations for which equilibrium cannot be achieved during the short time period of explosive eruptions.

## Acknowledgments

[57] We are grateful to A. Michel and V. Alaimo for help with chemical analyses, I. Cruz for the work performed on the Fogo A eruption, and M. Fialin and F. Couffignal for probe microanalyses. We thank different anonymous reviewers and V. Salters and J. Baker for their improvements to an earlier version of this paper in their editorial work. We also greatly thank D. R. Baker for scientific discussions and improvements to the English. Part of this work was performed thanks to ANR Volgaspec. IPGP contribution: 3015.

## References

- Aiuppa, A., D. R. Baker, and J. D. Webster (2009), Halogens in volcanic systems, *Chem. Geol.*, **263**, 1–18, doi:10.1016/j.chemgeo.2008.10.005.
- Allard, P., M. Burton, and Filippo Muré (2005), Spectroscopic evidence for lava fountain driven by previously accumulated magmatic gas, *Nature*, **433**, 407–410, doi:10.1038/nature03246.
- Alletti, M., D. R. Baker, and C. Freda (2007), Halogen diffusion in a basaltic melt, *Geochim. Cosmochim. Acta*, **71**, 3570–3580, doi:10.1016/j.gca.2007.04.018.
- Alletti, M., D. R. Baker, B. Scaillet, A. Aiuppa, R. Moretti, and L. Ottolini (2009), Chlorine partitioning between a basaltic melt and H<sub>2</sub>O–CO<sub>2</sub> fluids, *Chem. Geol.*, **263**, 37–50, doi:10.1016/j.chemgeo.2009.04.003.
- Anderko, A., and K. S. Pitzer (1993a), Equation of state representation of phase equilibria and volumetric properties of the system NaCl–H<sub>2</sub>O above 573K, *Geochim. Cosmochim. Acta*, **57**, 1657–1680, doi:10.1016/0016-7037(93)90105-6.
- Atlas, Z. D., J. E. Dixon, G. Sen, M. Finny, and A. L. Martin-Del Pozzo (2006), Melt inclusions from Volcán Popocatepetl and Volcán de Colima, Mexico: Melt evolution due to vapor-saturated crystallization during ascent, *J. Volcanol. Geotherm. Res.*, **153**, 221–240, doi:10.1016/j.jvolgeores.2005.06.010.
- Bai, T. B., and A. F. Koster van Groos (1994), Diffusion of chlorine in granitic melts, *Geochim. Cosmochim. Acta*, **58**, 113–123, doi:10.1016/0016-7037(94)90450-2.
- Baker, D. R. (2008), The fidelity of melt inclusions as records of melt composition, *Contrib. Mineral. Petrol.*, **156**(3), 377–395, doi:10.1007/s00410-008-0291-3.
- Balcone-Boissard, H., B. Villemant, G. Boudon, and A. Michel (2008), Non-volatile vs volatile behaviours of halogens during the AD 79 plinian eruption of Mt. Vesuvius, Italy, *Earth Planet. Sci. Lett.*, **269**(1–2), 66–79, doi:10.1016/j.epsl.2008.02.003.
- Balcone-Boissard, H., A. Michel, and B. Villemant (2009), Simultaneous determination of fluorine, chlorine, bromine and iodine in six geochemical reference materials using pyrohydrolysis, ion chromatography and inductively coupled plasma mass spectrometry, *Geostand. Geoanal. Res.*, **33**(4), 477–485, doi:10.1111/j.1751-908X.2009.00018.x.
- Blundy, J., and K. V. Cashman (2001), Magma ascent and crystallisation at Mount St Helens, 1980–1986, *Contrib. Mineral. Petrol.*, **140**, 631–650.
- Booth, B., R. Croasdale, and G. P. L. Walker (1978), A quantitative study of five thousand years of volcanism on Sao Miguel, Azores, *Philos. Trans. R. Soc. London, Ser. A*, **288**(1352), 271–319.
- Bureau, H., and N. Métrich (2003), An experimental study of bromine behaviour in water-saturated silicic melts, *Geochim. Cosmochim. Acta*, **67**(9), 1689–1697, doi:10.1016/S0016-7037(02)01339-X.
- Bureau, H., H. Keppler, and N. Métrich (2000), Volcanic degassing of bromine and iodine: Experimental fluid/melt partitioning data and applications to stratospheric chemistry, *Earth Planet. Sci. Lett.*, **183**, 51–60, doi:10.1016/S0012-821X(00)00258-2.
- Burnham, C. W. (1975), Water and magmas; a mixing model, *Geochim. Cosmochim. Acta*, **39**, 1077–1084, doi:10.1016/0016-7037(75)90050-2.
- Burnham, C. W. (1979), The importance of volatile constituents, in *The Evolution of the Igneous Rocks: Fiftieth Anniversary Appraisal*, edited by H. S. Yoder Jr., pp. 439–482, Princeton Univ. Press, Princeton, N. J.
- Burnham, C. W. (1994), Development of the Burnham model for prediction of the H<sub>2</sub>O solubility in magmas, in *Volatiles in Magmas, Rev. Mineral.*, vol. 30, edited by M. R. Carroll and J. R. Holloway, pp. 123–129, Mineral. Soc. of Am., Washington, D. C.
- Burton, M., H. M. Mader, and M. Polacci (2007), The role of gas percolation in quiescent degassing of persistently active basaltic volcanoes, *Earth Planet. Sci. Lett.*, **264**(1–2), 46–60, doi:10.1016/j.epsl.2007.08.028.
- Candela, P. A., and P. M. Piccoli (1995), Model ore-metal partitioning from melts into vapor and vapor/brine mixtures, in *Magmas, Fluids, and Ore Deposits, Mineral. Assoc. Can. Short Course Ser.*, vol. 23, edited by J. F. H. Thompson, pp. 101–127, Mineral. Assoc. of Canada, Quebec, Canada.
- Carroll, M. R. (2005), Chlorine solubility in evolved alkaline magmas, *Ann. Geophys.*, **48**(4/5), 619–631.
- Carroll, M. R., and J. G. Blank (1997), The solubility of H<sub>2</sub>O in phonolitic melts, *Am. Mineral.*, **82**, 549–556.
- Chai, J. Y., and Y. Muramatsu (2007), Determination of bromine and iodine in twenty-three geochemical reference materials by ICP-MS, *Geostand. Geoanal. Res.*, **31**(2), 143–150, doi:10.1111/j.1751-908X.2007.00856.x.
- Chevychelov, V. U., R. E. Botcharnikov, and F. Holtz (2008), Partitioning of Cl and F between fluid and hydrous phonolitic melt of Mt. Vesuvius at ~850–1000°C and 200 MPa, *Chem. Geol.*, **256**, 172–184, doi:10.1016/j.chemgeo.2008.06.025.

- Cioni, R. (2000), Volatile content and degassing processes in the AD 79 magma chamber at Vesuvius (Italy), *Contrib. Mineral. Petrol.*, **140**, 40–54, doi:10.1007/s004100000167.
- Cioni, R., L. Civetta, P. Marianelli, N. Metrich, R. Santacroce, and A. Sbrana (1995), Compositional layering and syn-eruptive mixing of a periodically refilled shallow magma chamber: The AD 79 plinian eruption of Vesuvius, *J. Petrol.*, **36**(3), 739–776.
- Clarke, A. B., S. Stephens, R. Teasdale, R. S. J. Sparks, and K. Diller (2007), Petrologic constraints on the decompression history of magma prior to Vulcanian explosions at the Soufrière Hills volcano, Montserrat, *J. Volcanol. Geotherm. Res.*, **161**, 261–274, doi:10.1016/j.jvolgeores.2006.11.007.
- Clocchiatti, R. (1975), Les inclusions vitreuses des cristaux de quartz Etude thermo-optique et chimique Applications géologiques, *Mem. Soc. Geol. Fr.*, **122**, 96 pp.
- Couch, S., R. S. J. Sparks, and M. R. Carroll (2003), The kinetics of degassing-induced crystallisation at Soufrière Hills volcano, *J. Petrol.*, **44**(8), 1477–1502, doi:10.1093/petrology/44.8.1477.
- Cruz, M. I., et al. (2004), Degassing processes during the Fogo A plinian eruption (São Miguel - Azores) (abstract), paper presented at the IAVCEI General Assembly, Int. Assoc. of Volcanol. and Chem. of the Earth's Inter., Pucón, Chile.
- Devine, J. D., and J. E. Gardner (1995), Comparison of micro-analytical methods for estimating H<sub>2</sub>O contents of silicic volcanic glasses, *Am. Mineral.*, **80**, 319–328.
- Di Matteo, V., M. R. Carroll, H. Behrens, F. Vetere, and R. A. Brooker (2004), Water solubility in trachytic melts, *Chem. Geol.*, **213**, 187–196, doi:10.1016/j.chemgeo.2004.08.042.
- Dingwell, D. B., C. Romano, and K.-U. Hess (1996), The effect of water on the viscosity of a haplogranitic melt under P-T-X conditions relevant to silicic volcanism, *Contrib. Mineral. Petrol.*, **124**(1), 19–28, doi:10.1007/s004100050170.
- Dreibus, G., B. Spettel, and H. Waenke (1979), Halogens in meteorites and their primordial abundances, in *Origin and Distribution of the Elements*, edited by L. H. Ahrens, pp. 33–38, Pergamon, Oxford, U. K.
- Dreibus, G., J. M. Friedrich, R. Haubold, W. Huisl, and B. Spettel (2004), Halogens, carbon, and sulfur in the Tagish Lake meteorite: Implications for classification and terrestrial alteration, *Lunar Planetary Sci.*, **XXXV**, Abstract 1268.
- Driesner, T., and C. Heinrich (2007), The system H<sub>2</sub>O–NaCl. Part I: Correlation formulae for phase relations in temperature–pressure–composition space from 0 to 1000°C, 0 to 5000 bar, and 0 to 1 XNaCl, *Geochim. Cosmochim. Acta*, **71**, 4880–4901, doi:10.1016/j.gca.2006.01.033.
- Druitt, T. H., et al. (2002), Episodes of cyclic vulcanian explosive activity with fountain collapse at Soufrière Hills volcano, Montserrat, in *The Eruption of Soufriere Hills Volcano, Montserrat (1995 to 1999)*, edited by T. H. Druitt and B. P. Kokelaar, *Geol. Soc. London Mem.*, **21**, 281–306.
- Eichelberger, J. C. (1995), Silicic volcanism: Ascent of viscous magmas from crustal reservoirs, *Annu. Rev. Earth Planet. Sci.*, **23**, 41–63, doi:10.1146/annurev.ea.23.050195.000353.
- Eichelberger, J. C., C. R. Carrigan, H. R. Westrich, and R. H. Price (1986), Non-explosive silicic volcanism, *Nature*, **323**, 598–602, doi:10.1038/323598a0.
- Gardner, J. E., R. M. E. Thomas, C. Jaupart, and S. Tait (1996), Fragmentation of magma during Plinian volcanic eruptions, *Bull. Volcanol.*, **58**, 144–162, doi:10.1007/s004450050132.
- Gardner, J. E., A. Burgisser, M. Hort, and M. Rutherford (2006), Experimental and model constraints on degassing of magma during ascent and eruption, in *Neogene-Quaternary Continental Margin Volcanism: A Perspective From Mexico*, edited by C. Siebe, J. L. Macias, and G. J. Aguirre-Diaz, *Spec. Pap. Geol. Soc. Am.*, **402**, 99–113, doi:10.1130/2006.2402(04).
- Giggenbach, W. F. (1996), Chemical composition of volcanic gases, in *Monitoring and Mitigation of Volcanic Hazards*, edited by R. Scarpa and R. I. Tilling, pp. 221–256, Springer Verlag, New York.
- Giordano, D., J. K. Russell, and D. B. Dingwell (2008), Viscosity of magmatic liquids: A model, *Earth Planet. Sci. Lett.*, **271**, 123–134, doi:10.1016/j.epsl.2008.03.038.
- Goles, G. G., and L. P. Greenland (1966), Estimates of primordial halogen abundance ratios from studies of chondritic meteorites, *Astron. J.*, **71**, 162, doi:10.1086/110128.
- Gurioli, L., B. F. Houghton, K. V. Cashman, and R. Cioni (2005), Complex changes in eruption dynamics during the 79 AD eruption of Vesuvius, *Bull. Volcanol.*, **67**, 144–159, doi:10.1007/s00445-004-0368-4.
- Hammer, J. E., K. V. Cashman, R. P. Hoblitt, and S. Newman (1999), Degassing and microlite crystallisation during pre-climatic events of the 1991 eruption of Mt. Pinatubo, Philippines, *Bull. Volcanol.*, **60**, 355–380, doi:10.1007/s004450050238.
- Harris, A. J. L., W. Rose, and L. Flynn (2003), Temporal trends in lava dome extrusion at Santiaguito 1922–2000, *Bull. Volcanol.*, **65**, 77–89, doi:10.1007/s00445-002-0243-0.
- Humphreys, M. C. S., M. Edmonds, T. Christopher, and V. Hards (2009), Chlorine variations in the magma of Soufrière Hills Volcano, Montserrat: Insights from Cl in hornblende and melt inclusions, *Geochim. Cosmochim. Acta*, **73**, 5693–5708, doi:10.1016/j.gca.2009.06.014.
- Iacono-Marziano, G., B. C. Schmidt, and D. Dolfi (2007), Equilibrium and disequilibrium degassing of a phonolitic melt (Vesuvius AD 79 “white pumice”) simulated by decompression experiments, *J. Volcanol. Geotherm. Res.*, **161**, 151–164, doi:10.1016/j.jvolgeores.2006.12.001.
- Jambon, A., B. Dérulle, G. Dreibus, and F. Pineau (1995), Chlorine and bromine abundance in MORB: The contrasting behaviour of the Mid-Atlantic Ridge and East Pacific Rise and implications for chlorine geodynamic cycle, *Chem. Geol.*, **126**, 101–117, doi:10.1016/0009-2541(95)00112-4.
- Jaupart, C., and C. J. Allègre (1991), Gas content, eruption rate and instabilities in silicic volcanoes, *Earth Planet. Sci. Lett.*, **102**, 413–429, doi:10.1016/0012-821X(91)90032-D.
- Kaminski, E., and C. Jaupart (1997), Expansion and quenching of vesicular magma fragments in Plinian eruptions, *J. Geophys. Res.*, **102**(B6), 12,187–12,203, doi:10.1029/97JB00622.
- Kent, A. J. R., D. W. Peate, S. Newman, E. M. Stolper, and J. A. Pearce (2002), Chlorine in submarine glasses from the Lau Basin: Seawater contamination and constraints on the composition of slab-derived fluids, *Earth Planet. Sci. Lett.*, **202**, 361–377, doi:10.1016/S0012-821X(02)00786-0.
- Kilinc, I. A., and C. W. Burnham (1972), Partitioning of chloride between silicate melts and coexisting aqueous phase from 2 to 8 kbars, *Earth Planet. Sci. Lett.*, **102**, 413–429.
- Kravchuk, I. F., and H. Keppler (1994), Distribution of chloride between aqueous fluids and felsic melts at 2 kbar and 800°C, *Eur. J. Mineral.*, **6**, 913–923.
- Liebscher, A. (2007), Experimental studies in model fluid systems, *Rev. Mineral. Geochem.*, **65**, 15–47, doi:10.2138/rmg.2007.65.2.
- Liu, Y., Y. Zhanga, and H. Behrens (2005), Solubility of H<sub>2</sub>O in rhyolitic melts at low pressures and a new empirical model for mixed H<sub>2</sub>O–CO<sub>2</sub> solubility in rhyolitic melts,



- J. Volcanol. Geotherm. Res.*, 143(1–3), 219–235, doi:10.1016/j.jvolgeores.2004.09.019.
- Lowenstern, J. B. (1994), Chlorine, fluid immiscibility and degassing in peralkaline magmas from Pantelleria, Italy, *Am. Mineral.*, 79, 353–369.
- Lowenstern, J. B. (1995), Applications of silicate melt inclusions to the study of magmatic volatiles, in *Magmas, Fluids, and Ore Deposits*, Mineral. Assoc. Can. Short Course Ser., vol. 23, edited by J. F. H. Thompson, pp. 71–99, Mineral. Assoc. of Canada, Quebec, Canada.
- Martel, C., M. Pichavant, J.-L. Bourdier, H. Traineau, F. Holtz, and B. Scaillet (1998), Magma storage and control of eruption regime in silicic volcanoes: Experimental evidence from Mt. Pelée, *Earth Planet. Sci. Lett.*, 156, 89–99, doi:10.1016/S0012-821X(98)00003-X.
- Melnik, O., and R. S. J. Sparks (1999), Nonlinear dynamics of lava dome extrusion, *Nature*, 402, 37–41, doi:10.1038/46950.
- Melnik, O., and R. S. J. Sparks (2002), Dynamics of magma ascent and lava extrusion at Soufrière Hills Volcano, Montserrat, in *The Eruption of Soufrière Hills Volcano, Montserrat (1995 to 1999)*, edited by T. H. Druitt and B. P. Kokelaar, *Geol. Soc. London Mem.*, 21, 153–172.
- Métrich, N., and M. J. Rutherford (1992), Experimental study of chlorine behavior in hydrous silicic melts, *Geochim. Cosmochim. Acta*, 56, 607–616, doi:10.1016/0016-7037(92)90085-W.
- Michel, A., and B. Villemant (2003), Determination of halogens (F, Cl, Br, I), sulfur and water in seventeen geological reference materials, *Geostand. Geoanal. Res.*, 27, 163–171, doi:10.1111/j.1751-908X.2003.tb00643.x.
- Moore, R. B. (1990), Volcanic geology and eruption frequency, São Miguel, Azores, *Bull. Volcanol.*, 52(8), 602–614, doi:10.1007/BF00301211.
- Moretti, R., P. Papale, and G. Ottonello (2003), A model for the saturation of C–O–H–S fluids in silicate melts, in *Volcanic Degassing*, edited by C. Oppenheimer, D. M. Pyle, and J. Barclay, *Geol. Soc. Spec. Publ.*, 213, 81–101.
- Morizet, Y., R. A. Brooker, and S. C. Kohn (2002), CO<sub>2</sub> in haplo-phonolite melt: Solubility, speciation and carbonate complexation, *Geochim. Cosmochim. Acta*, 66(10), 1809–1820, doi:10.1016/S0016-7037(01)00893-6.
- Oppenheimer, C., V. I. Tsanev, C. F. Braban, R. A. Cox, J. W. Adams, A. Aiuppa, N. Bobrowski, P. Delmelle, J. Barclay, and A. J. S. McGonigle (2006), BrO formation in volcanic plumes, *Geochim. Cosmochim. Acta*, 70, 2935–2941, doi:10.1016/j.gca.2006.04.001.
- Papale, P., A. Neri, and G. Macedonio (1998), The role of magma composition and water content in explosive eruptions: 1. Conduit ascent dynamics, *J. Volcanol. Geotherm. Res.*, 87, 75–93, doi:10.1016/S0377-0273(98)00101-2.
- Robertson, R., et al. (1998), The explosive eruption of Soufrière Hills Volcano, Montserrat, West Indies, 17 September 1996, *Geophys. Res. Lett.*, 25(18), 3429–3432, doi:10.1029/98GL01442.
- Robertson, R., W. P. Aspinall, R. A. Herd, G. E. Norton, R. S. J. Sparks, and S. R. Young (2000), The 1995–1998 eruption of the Soufrière Hills Volcano, Montserrat, West Indies, *Philos. Trans. R. Soc. London, Ser. A*, 358, 1619–1637, doi:10.1098/rsta.2000.0607.
- Rose, W. I. (1972a), Notes on the 1902 eruption of Santa Maria Volcano, Guatemala, *Bull. Volcanol.*, 36, 29–45, doi:10.1007/BF02596981.
- Rose, W. I. (1972b), Pattern and mechanism of volcanic activity at the Santiaguito volcanic dome, *Bull. Volcanol.*, 36, 73–94.
- Schilling, J. G., M. B. Bergeron, R. Evans, and J. V. Smith (1980), Halogens in the mantle beneath the North Atlantic, *Philos. Trans. R. Soc. London, Ser. A*, 297, 147–178, doi:10.1098/rsta.1980.0208.
- Shinohara, H. (1994), Exsolution of immiscible vapor and liquid phases from a crystallizing silicate melt: Implications for chlorine and metal transport, *Geochim. Cosmochim. Acta*, 58, 5215–5221, doi:10.1016/0016-7037(94)90306-9.
- Shinohara, H. (2009), A missing link between volcanic degassing and experimental studies on chloride partitioning, *Chem. Geol.*, 263, 51–59, doi:10.1016/j.chemgeo.2008.12.001.
- Shinohara, H., J. T. Iiyama, and S. Matsuo (1989), Partition of chlorine compounds between silicate melt and hydrothermal solutions, *Geochim. Cosmochim. Acta*, 53, 2617–2630, doi:10.1016/0016-7037(89)90133-6.
- Signorelli, S., and B. Capaccioni (1999), Behaviour of chlorine prior and during the 79 A.D. Plinian eruption of Vesuvius (southern Italy) as inferred from the present distribution in glassy mesostase and whole-pumices, *Lithos*, 46, 715–730, doi:10.1016/S0024-4937(98)00092-9.
- Signorelli, S., and M. R. Carroll (2000), Solubility and fluid-melt partitioning of Cl in hydrous phonolitic melts, *Geochim. Cosmochim. Acta*, 64(16), 2851–2862, doi:10.1016/S0016-7037(00)00386-0.
- Sigurdsson, H., W. Cornell, and S. Carey (1990), Influence of magma withdrawal on compositional gradients during the AD 79 Vesuvius eruption, *Nature*, 345, 519–521, doi:10.1038/345519a0.
- Snyder, D. C., E. Widom, A. J. Pietruszka, and R. W. Carlson (2004), The role of open-system processes in the development of silicic magma chambers: A chemical and isotopic investigation of the Fogo A trachyte deposit, São Miguel Azores, *J. Petrol.*, 45, 723–738, doi:10.1093/petrology/egg104.
- Snyder, D. C., E. Widom, A. J. Pietruszka, R. W. Carlson, and H.-U. Schmincke (2007), Time scales of formation of zoned magma chambers: U-series disequilibria in the Fogo A and 1563 A.D. trachyte deposits, São Miguel, Azores, *Chem. Geol.*, 239(1–2), 138–155, doi:10.1016/j.chemgeo.2007.01.002.
- Sourirajan, S., and G. C. Kennedy (1962), The system H<sub>2</sub>O–NaCl at elevated temperatures and pressures, *Am. J. Sci.*, 260, 115–141.
- Sparks, R. S. J. (2003), Dynamics of magma degassing, in *Volcanic Degassing*, edited by C. Oppenheimer, D. M. Pyle, and J. Barclay, *Geol. Soc. Spec. Publ.*, 213, 5–22, doi:10.1144/GSL.SP.2003.213.01.02.
- Sparks, R. S. J., et al. (1998), Magma production and growth of the lava dome of the Soufrière Hills volcano, Montserrat: November 1995 to December 1997, *Geophys. Res. Lett.*, 25, 3421–3424, doi:10.1029/98GL00639.
- Straub, S. M., and G. D. Layne (2003), The systematics of chlorine, fluorine, and water in Izu arc front volcanic rocks: Implications for volatile recycling in subduction zones, *Geochim. Cosmochim. Acta*, 67(21), 4179–4203, doi:10.1016/S0016-7037(03)00307-7.
- Thomas, N., C. Jaupart, and S. Vergnolle (1994), On the vesicularity of pumice, *J. Geophys. Res.*, 99(B8), 15,633–15,644, doi:10.1029/94JB00650.
- Villemant, B., and G. Boudon (1998), Transition between dome-forming and plinian eruptive style: H<sub>2</sub>O and Cl degassing behaviour, *Nature*, 392, 65–69, doi:10.1038/32144.
- Villemant, B., and G. Boudon (1999), H<sub>2</sub>O and halogen (F, Cl, Br) behaviour during shallow magma degassing processes,

- Earth Planet. Sci. Lett.*, **168**, 271–286, doi:10.1016/S0012-821X(99)00058-8.
- Villemant, B., G. Boudon, and J.-C. Komorowski (1996), U-series disequilibrium in arc magmas induced by water-magma interaction, *Earth Planet. Sci. Lett.*, **140**(1–4), 259–267, doi:10.1016/0012-821X(96)00035-0.
- Villemant, B., G. Boudon, S. Nougriat, S. Poteaux, and A. Michel (2003), Water and halogens in volcanic clasts: Tracers of degassing processes during plinian and dome-building eruptions, in *Volcanic Degassing*, edited by C. Oppenheimer, D. M. Pyle, and J. Barclay, *Geol. Soc. Spec. Publ.*, **213**, 63–79, doi:10.1144/GSL.SP.2003.213.01.05.
- Villemant, B., J. Mouatt, and A. Michel (2008), Andesitic magma degassing investigated through H<sub>2</sub>O vapour–melt partitioning of halogens at Soufrière Hills Volcano, Montserrat (Lesser Antilles), *Earth Planet. Sci. Lett.*, **269**, 212–229, doi:10.1016/j.epsl.2008.02.014.
- Voight, B., et al. (1999), Magma flow instability and cyclic activity at Soufrière Hills volcano, Montserrat, British 700 West Indies, *Science*, **283**, 1138–1142, doi:10.1126/science.283.5405.1138.
- Walker, G. P. L., and R. Croasdale (1971), Two Plinian-type eruptions in the Azores, *J. Geol. Soc.*, **127**, 17–55, doi:10.1144/gsjgs.127.1.0017.
- Wallace, P. J. (2005), Volatiles in subduction zone magmas: Concentrations and fluxes based on melt inclusion and volcanic gas data, *J. Volcanol. Geotherm. Res.*, **140**, 217–240, doi:10.1016/j.jvolgeores.2004.07.023.
- Watanabe, S., E. Widom, N. Wallenstein, and D. Snyder (2005), The evolution of chemically zoned trachytic deposits: Comparisons of Fogo A and Fogo 1563AD, São Miguel, Azores, *Geochim. Cosmochim. Acta*, **69**(10), 245.
- Watson, E. B. (1994), Diffusion in volatile-bearing magmas, in *Volatiles in Magmas*, *Rev. Mineral.*, vol. 30, edited by M. R. Carroll and J. R. Holloway, pp. 371–411, Mineral. Soc. of Am., Washington, D. C.
- Webster, J. D. (1992a), Fluid-melt interactions in Cl-rich granitic systems: Effects of melt composition at 2 kbar and 800 °C, *Geochim. Cosmochim. Acta*, **56**, 659–678, doi:10.1016/0016-7037(92)90088-Z.
- Webster, J. D. (1997), Chloride solubility in felsic melts and the role of chloride in magmatic degassing, *J. Petrol.*, **38**, 1793–1807, doi:10.1093/petrology/38.12.1793.
- Webster, J. D., and J. R. Holloway (1988), Experimental constraints on the partitioning of Cl between topaz rhyolite melt and H<sub>2</sub>O and H<sub>2</sub>O + CO<sub>2</sub> fluids: New implications for granitic differentiation and ore deposition, *Geochim. Cosmochim. Acta*, **52**, 2091–2105, doi:10.1016/0016-7037(88)90189-5.
- Webster, J. D., and C. R. Rebbert (1998), Experimental investigation of H<sub>2</sub>O and Cl<sup>−</sup> solubilities in F-enriched silicate liquids; implications for volatile saturation of topaz rhyolite magmas, *Contrib. Mineral. Petrol.*, **132**, 198–207, doi:10.1007/s004100050416.
- Webster, J. D., R. J. Kinzler, and E. A. Mathez (1999), Chloride and water solubility in basalt and andesitic melts and implications for magmatic degassing, *Geochim. Cosmochim. Acta*, **63**, 729–738, doi:10.1016/S0016-7037(99)00043-5.
- Widom, E., H.-U. Schmincke, and J. B. Gill (1992), Processes and time scales in the evolution of a chemically zoned trachyte: Fogo A, São Miguel, Azores, *Contrib. Mineral. Petrol.*, **111**, 311–328, doi:10.1007/BF00311194.
- Williams, S. N., and S. Self (1983), The October 1902 plinian eruption of Santa Maria volcano, Guatemala, *J. Volcanol. Geotherm. Res.*, **16**(1–2), 33–56, doi:10.1016/0377-0273(83)90083-5.
- Wolff, J. A., and M. Storey (1983), The volatile component of some pumice-forming alkaline magmas from the Azores and Canary islands, *Contrib. Mineral. Petrol.*, **82**, 66–74, doi:10.1007/BF00371176.
- Zhang, Y. (1999), H<sub>2</sub>O in rhyolitic glasses and melts: Measurements speciation solubility and diffusion, *Rev. Geophys.*, **37**, 493–516, doi:10.1029/1999RG900012.
- Zhang, Y., E. M. Stolper, and G. J. Wasserburg (1991), Diffusion of water in rhyolitic glasses, *Geochim. Cosmochim. Acta*, **55**, 441–456, doi:10.1016/0016-7037(91)90003-N.